

# Photochemistry of the sea-surface microlayer (SML) influenced by a phytoplankton bloom: A mesocosm study

5 Olenka Jibaja Valderrama, Daniele Scheres Firak, Thomas Schaefer, Manuela van Pinxteren, Khannah Wadinga Fomba, Hartmut Herrmann\*

Atmospheric Chemistry Department (ACD), Leibniz-Institute for Tropospheric Research (TROPOS), Leipzig, 04318, Germany

\*Correspondence to: Hartmut Herrmann ([herrmann@tropos.de](mailto:herrmann@tropos.de))

10 Submitted to:  
\*\*\*\*\* Biogeosciences \*\*\*\*\*  
~~February 2026~~ August 2025

15 **Abstract.** The sea-surface microlayer (SML) is the thin boundary interface between the ocean and the atmosphere, and it is expected to play a crucial role in atmospheric chemistry on a global scale. Being a biologically-enriched environment exposed to strong actinic radiation, the SML is potentially a hotspot for photochemical reactions that have relevance in the transformation and cycling of organic compounds. The present study explores the photochemical production and degradation of carbonyl compounds, as well as the photochemical oxidation capacity in both ambient SML and underlying water (ULW)  
20 samples. Natural seawater samples were collected during a mesocosm study where a phytoplankton bloom was induced through the controlled addition of inorganic nutrients. To assess the photochemistry of carbonyl compounds, collected SML and ULW samples were irradiated for 5 hours. The photochemical formation and degradation of 17 carbonyl compounds were quantified by monitoring compound-specific changes in concentrations, which varied significantly across the samples. Before irradiation, values in the SML ranged from 201 to 762 nmol L<sup>-1</sup> in the pre-bloom phase, 984 to 4591 nmol L<sup>-1</sup> in the bloom  
25 phase, and 647 to 4894 nmol L<sup>-1</sup> in the post-bloom phase; while in the ULW they were significantly lower (e.g., 136 to 366 nmol L<sup>-1</sup> in the bloom phase). After 5 hours of irradiation, the concentrations of carbonyl compounds increased further, reaching up to 6026 nmol L<sup>-1</sup> in the SML during the bloom phase and 419 nmol L<sup>-1</sup> in the ULW. Experimental evidence suggests an enhanced photochemical activity in the SML during the bloom phase for glyoxal, methylglyoxal, methyl vinyl ketone (MVK), methacrolein, acrolein, crotonaldehyde, heptanal, biacetyl, hexanal and trans-2-hexenal. The observed  
30 photooxidation capacity of the seawater samples indicate a dominant influence of redox active species like metal ions, rather than of the phytoplankton bloom phases. The overall photochemical oxidation capacity was similar for both SML and ULW samples, with average values of 34 μM s<sup>-1</sup>. Our findings show an influence of biological activity in the photochemistry of

carbonyl compounds in the SML and its implications for the emission of volatile organic compounds (VOCs) to the marine atmosphere, pointing to the complex interaction of biotic and abiotic factors in the air-sea boundary and underscoring the relevance of marine photochemistry in biogeochemical processes.

## 1 Introduction

The sea-surface microlayer (SML) is the uppermost boundary layer of the ocean. With a thickness typically between 1 and 1000  $\mu\text{m}$ , the SML potentially covers up to 70 % of the Earth's surface (Wurl et al., 2017; Wurl et al., 2011; Wurl et al., 2016; Hardy, 1982). This specific environment is characterized by its enrichment ~~both~~ in dissolved organic matter (DOM), particulate organic matter (POM) and inorganic matter, and its direct exposure to solar radiation, both factors presumably leading to photochemical transformations that result in a diverse mixture of chemical compounds (Hardy, 1982; Zafiriou, 1977). The SML naturally acts as an interface between the underlying water (ULW) and the atmosphere, and many transfer processes, such as those involving particles or trace gases, ~~are~~ mediated through the SML and its respective properties (Wurl et al., 2017; Engel et al., 2017). Clearly, based on its biological, chemical and physical properties, the SML can be distinguished from ULW.

The DOM present in the SML includes carbohydrates, lipids, amino acids, proteins and humic substances, which are primarily produced by marine biota during phytoplankton growth, grazing and viral lysis (Lampert, 1978; Lancelot, 1979; Hansell and Carlson, 2002; Liss et al., 1997; Carpenter and Nightingale, 2015). A portion of the total DOM, the coloured dissolved organic matter (CDOM), absorbs light in the ultraviolet and visible region, leading to photochemical transformation and production of reactive species (Coble, 2007; Rochelle-Newall et al., 1999). The SML also has light-absorbing molecules that transfer energy to other compounds and trigger photochemical transformations, known as photosensitizers (Mopper and Stahovec, 1986; Momzikoff et al., 1983). Photosensitizers do not only enhance photochemical reactions in seawater, but their decay releases fragments of photosynthetic structures rich in pigments that may also undergo photochemical degradation (Zafiriou, 1977).

Under exposure to sunlight, CDOM and humic substances in seawater undergo photochemical reactions that form species like carbonyl compounds. Field-based measurements provided evidence of oceanic production of aldehydes like formaldehyde, acetaldehyde, glyoxal, methylglyoxal, propanal, and hexanal; and ketones like acetone (de Bruyn et al., 2011; Kieber et al., 1990; Mopper and Stahovec, 1986; Mopper et al., 1991; van Pinxteren and Herrmann, 2013; Zhu and Kieber, 2019, 2018). However, there are still considerable doubts regarding the rates in which these processes occur and their interplay with biological events. Furthermore, investigations on the photochemistry in seawater of additional carbonyl compounds with potential relevance in the marine environment are, to this moment, still limited.

Carbonyl compounds serve as energy sources for marine microorganisms (de Bruyn et al., 2017; Dixon et al., 2014). Due to their high volatility, carbonyl compounds produced in the SML are also potential precursors of oxygenated volatile organic compounds (OVOCs) in the marine atmosphere. OVOCs can contribute to the formation of free radicals and secondary organic aerosols (SOAs), therefore impacting air quality, the atmospheric oxidative capacity and cloud formation.

65 Photochemistry in the SML plays a critical role in global biogeochemistry by influencing marine carbon cycling and atmospheric chemistry in the marine environment (Tinel et al., 2023). Both the fate of DOM and the formation of volatile organic compounds (VOCs) in seawater are highly impacted by its photochemical oxidation capacity, governed by the sunlight-driven production of excited triplet-state CDOM ( $^3\text{CDOM}^*$ ) and reactive oxidants. These processes occur alongside or even exceed biological pathways of transformation of DOM (Andrews et al., 2000). Earlier research demonstrated the production of important oxidants such as hydroxyl radicals (OH), superoxide radicals ( $\text{O}_2^-$ ), singlet oxygen ( $^1\text{O}_2$ ), excited state DOM triplets and hydrogen peroxide ( $\text{H}_2\text{O}_2$ ) (Fujii and Otani, 2017; Scully et al., 1996; Zhang et al., 2012; Dalrymple et al., 2010; Sun et al., 2015; Vaughan and Blough, 1998; Waggoner et al., 2017; Chu et al., 2015; Grandbois et al., 2008; McNeill and Canonica, 2016; Berg et al., 2019) through the photolysis of DOM in environmental waters. The production and consumption of these oxidants in natural waters is enhanced in the presence of trace metals, such as copper (Cu) and iron (Fe) through redox reactions (Jomova and Valko, 2011; Millero et al., 1991; Sharma and Millero, 1988; González-Davila et al., 2004; Millero et al., 1987; Moffett and Zika, 1983, 1987). High concentrations of these metals have been observed in different regions of the North Sea (Balls, 1985; Siems et al., 2024; Duinker and Nolting, 1982; Nolting, 1986; Mart and Nurnberg, 1986), so the estimation the photochemical production of reactive oxidants is of high importance in the present study to get more insights into the oxidative potential of this interface.

80 Biological activity can also influence photochemical processes in the surface of the oceans. Phytoplankton blooms refer to the rapid increase in microscopic algae in the upper layer of the sea, produced by both natural processes and nutrient enrichment from anthropogenic eutrophication (Dai et al., 2023). Recent scientific evidence revealed that the higher biological activity during a phytoplankton bloom and the subsequent algal decay have an impact on chemical properties and reactivity in the SML, as the organic matter (OM) accumulated in the air-sea interface can undergo photochemical changes due to excited triplet-state and radical-driven oxidation. For instance, there is a clear connection between marine microbiological processes and glyoxal production, especially in the terminal phase of an algal bloom (Williams et al., 2024). Nevertheless, integrated, compound-specific studies connecting the photochemistry of carbonyl compounds in different phases of algal blooms and the photooxidation potential of the SML remain insufficient.

In the present work, the photochemical activity of SML and ULW was investigated for samples collected during a mesocosm study in which a phytoplankton bloom was induced by the controlled addition of inorganic nutrients. The photochemistry of the seawater samples was assessed through the compound-specific concentration changes of carbonyl compounds before and after irradiation, alongside measurements of the photooxidation capacity to elucidate potential formation and degradation pathways of seawater samples at different bloom stages. The 17 carbonyl compounds analysed in the present study were acetophenone, acrolein, benzaldehyde, biacetyl, butanal, crotonaldehyde, glyoxal, heptanal, hexanal, isovaleraldehyde, methacrolein, methylglyoxal, methyl vinyl ketone (MVK), octanal, propanal, trans-2-hexenal and trans,trans-2,4-hexadienal.

95 Even though acetaldehyde and acetone were initially also considered as target compounds, they were ultimately excluded from the final quantitative analysis since their calibration curves showed poor linearity, likely related to their high volatility and potential background contamination from laboratory air. Formaldehyde was not analysed in the current study. Experimental

evidence of enhanced photochemical activity of carbonyl compounds in the SML relative to the ULW is provided, particularly in periods of higher biological productivity, thereby offering new insights to integrate biological processes and photochemistry in the air-sea boundary.

## 2 Materials and methods

### 2.1 Seawater sampling during the field campaign

Ambient SML and ~~ULW underlying water~~ (40 cm depth) samples were collected during a mesocosm experiment conducted at Sea-sURface Facility (SURF), located at [the Institute of Chemistry and Biology of the Marine Environment \(ICBM\)](#) in Wilhelmshaven (Germany), between May 18<sup>th</sup> and June 16<sup>th</sup>, 2023. SML samples were collected daily using the glass plate technique (Harvey and Burzell, 1972), while ULW samples were obtained via suction using a syringe connected to a polypropylene tube submerged to 40 cm.

A controlled phytoplankton bloom was induced through the stepwise addition of inorganic nutrients: silicate and phosphorous (19.8  $\mu\text{mol L}^{-1}$  and 1.2  $\mu\text{mol L}^{-1}$ ) were added on May 26<sup>th</sup>; silicate, nitrogen and phosphorous (10  $\mu\text{mol L}^{-1}$ , 10  $\mu\text{mol L}^{-1}$  and 0.6  $\mu\text{mol L}^{-1}$ ) on May 30<sup>th</sup>, and nitrogen and phosphorous (5  $\mu\text{mol L}^{-1}$  and 0.3  $\mu\text{mol L}^{-1}$ ) on June 1<sup>st</sup> (Bibi et al., 2025). Based on chlorophyll *a* concentrations monitored in the ULW, three distinct bloom phases were defined:

- (1) an initial pre-bloom phase, with lower chlorophyll *a* levels ([average: 2.2  \$\mu\text{g L}^{-1}\$](#) ) prior to nutrient addition (May 18<sup>th</sup> to May 26<sup>th</sup>);
- (2) a nutrient-induced bloom phase, (May 27<sup>th</sup> to June 4<sup>th</sup>), characterized by a rapid increase in phytoplankton mass ([average: 7.3  \$\mu\text{g L}^{-1}\$](#) );
- (3) a post-bloom phase, marked by the gradual decline in phytoplankton biomass ([average: 1.8  \$\mu\text{g L}^{-1}\$](#) ) (June 5<sup>th</sup> to June 16<sup>th</sup>). ~~The bloom consisted on an initial bloom where *Emiliana huxleyi* (coccolithophore) was dominant, and a subsequent bloom of *Cylindrotheca Closterium* (diatoms) was had higher relevance (Fig. 1) (Bibi et al., 2025). Dissolved organic carbon (DOC) concentrations increased during the phytoplankton bloom phase, and remained elevated in the post bloom phase of the study. The concentrations of other phytoplankton pigments in the ULW samples followed similar trends to the ones reported for chlorophyll *a*. Concentrations of chlorophyll *c*, a photosynthetic pigment present in haptophytes ranged between 0.07 and 2.10  $\mu\text{g L}^{-1}$ , peaking on May 28<sup>th</sup>, June 1<sup>st</sup> and June 3<sup>rd</sup>. Chlorophyll *b* and  $\beta$ -carotene were found between 0.04 and 0.40  $\mu\text{g L}^{-1}$ , and 0.04 and 0.30  $\mu\text{g L}^{-1}$ , respectively. Even though chlorophyll *b* and  $\beta$ -carotene seemed to have a minor contribution to the total phytoplankton mass, they also experienced an increase that reached maximum values between June 1<sup>st</sup> and June 3<sup>rd</sup>. Overall, the observed trends support the presence of a nutrient-driven phytoplankton bloom, which consisted on an initial dominance of *Emiliana huxleyi* (coccolithophore), followed by a subsequent growth of *Cylindrotheca Closterium* (diatoms) (Fig. 1) (Bibi et al., 2025). To further contextualize the biological development of the mesocosm, dissolved organic carbon (DOC) and particulate organic carbon (POC) concentrations were also analysed. DOC concentrations ranged from 254 to 583  $\mu\text{mol L}^{-1}$  in the SML, and from 207 to 373  $\mu\text{mol L}^{-1}$  in ULW. DOC concentrations increased during the phytoplankton bloom phase, and~~

remained elevated in the post-bloom phase of the study. On the other hand, POC concentrations measured in the ULW samples were between 23 to 173  $\mu\text{mol L}^{-1}$ , and their temporal trend along the mesocosm study was comparable to that of the chlorophyll *a* concentrations. In terms of bacterial abundance, which includes both free bacteria and bacteria-like material, it peaked in the post-bloom stage and ranged from  $481 \times 10^6$  to  $1468 \times 10^6$  in the SML, and from  $245 \times 10^6$  to  $1681 \times 10^6$  in the ULW. An enrichment factor (EF) of  $1.3 \pm 0.7$  was found during the phytoplankton bloom. A detailed characterization of the biological parameters measured in this mesocosm study is provided by Bibi et al. (2025).

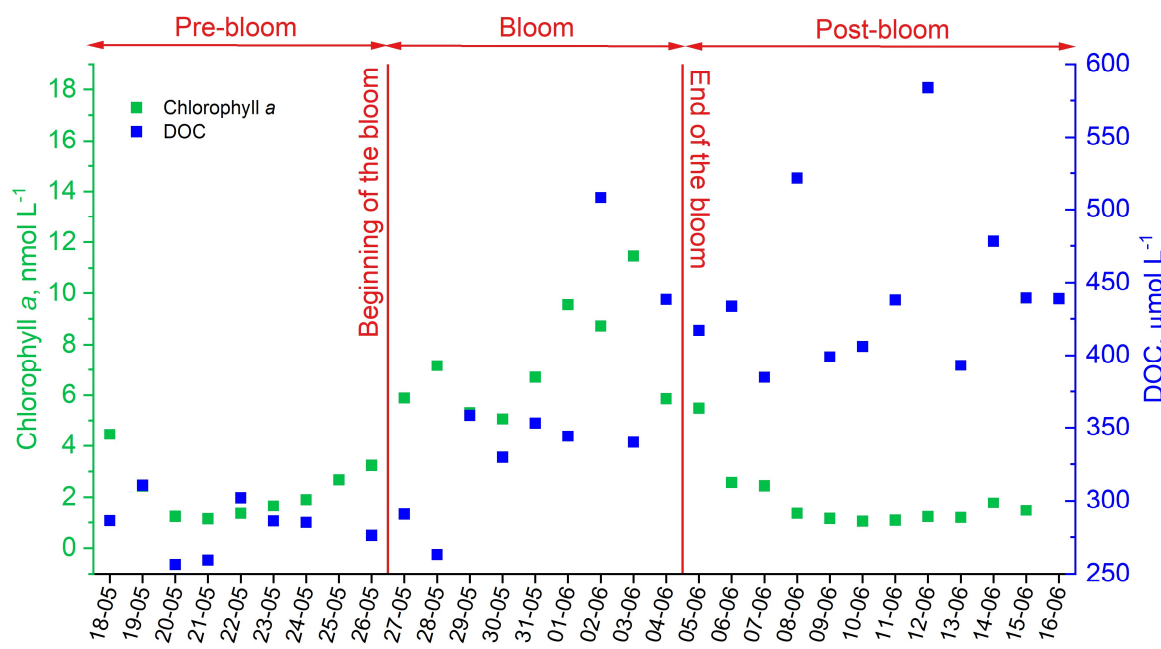


Figure 1: Chlorophyll *a* (monitored in the ULW) and DOC concentrations (monitored in the SML)ULW along the mesocosm experiment. Based on the chlorophyll *a* concentrations, three phytoplankton bloom phases were defined: pre-bloom, bloom and post-bloom (Adapted from Bibi et al., 2025).

A detailed description of the mesocosm setup, and the operational and sampling protocols are also available in Bibi et al. (2025). Collected SML and ULW samples were stored in sterile bottles at  $-20^{\circ}\text{C}$  until laboratory analysis. All experiments were conducted using unfiltered samples in order to preserve as much as possible their natural complexity, and the results therefore reflect the combined photochemical processes involving both DOM and POM. A total of 20 different seawater samples, 12 from the SML and eight from the ULW, were selected to represent the three bloom phases (Table 1) for the investigations of carbonyl compound photochemistry. Their photochemical reactivity was analysed using methods described in the following sections. Samples from May 20<sup>th</sup> and June 2<sup>nd</sup> were also considered for trace metals analysis.

Table 1: Overview of selected SML and ULW samples from the mesocosm analysed in this study for carbonyl compound photochemistry investigations

Seawater sample name	Type of sample	Sampling date	Sampling time (local time)	Salinity (PSU)	Bloom phase
SML-5*	SML	May 20 <sup>th</sup> , 2023	06:45	29.44	Pre-bloom
ULW-5*	ULW	May 20 <sup>th</sup> , 2023	06:45	29.49	Pre-bloom
SML-7	SML	May 22 <sup>nd</sup> , 2023	06:27	29.59	Pre-bloom
SML-8	SML	May 23 <sup>rd</sup> , 2023	15:16	29.66	Pre-bloom
SML-11	SML	May 26 <sup>th</sup> , 2023	06:20	29.87	Pre-bloom
ULW-11	ULW	May 26 <sup>th</sup> , 2023	06:20	29.92	Pre-bloom
SML-12	SML	May 27 <sup>th</sup> , 2023	15:35	29.91	Bloom
SML-13	SML	May 28 <sup>th</sup> , 2023	07:10	29.95	Bloom
ULW-13	ULW	May 28 <sup>th</sup> , 2023	07:10	30.00	Bloom
SML-15	SML	May 30 <sup>th</sup> , 2023	05:50	30.16	Bloom
ULW-15	ULW	May 30 <sup>th</sup> , 2023	05:50	30.29	Bloom
SML-17	SML	June 1 <sup>st</sup> , 2023	06:14	30.25	Bloom
ULW-17	ULW	June 1 <sup>st</sup> , 2023	06:14	30.30	Bloom
SML-18*	SML	June 2 <sup>nd</sup> , 2023	15:07	30.35	Bloom
ULW-18*	ULW	June 2 <sup>nd</sup> , 2023	15:07	30.38	Bloom
SML-23	SML	June 7 <sup>th</sup> , 2023	05:30	30.86	Post-bloom
SML-24	SML	June 8 <sup>th</sup> , 2023	14:59	31.01	Post-bloom
ULW-24	ULW	June 8 <sup>th</sup> , 2023	14:59	31.04	Post-bloom
SML-27	SML	June 11 <sup>th</sup> , 2023	05:30	31.31	Post-bloom
ULW-27	ULW	June 11 <sup>th</sup> , 2023	05:30	31.35	Post-bloom

Adapted from Bibi et al., 2025

\*Samples used for trace metals analysis

## 2.2 Photochemical reactor

155 For carbonyl compound photochemistry investigations, ambient SML and ULW samples were irradiated for 5 hours with a light source that simulated the actinic radiation in the sea surface. ~~in a~~ jacketed, temperature-controlled ( $25 \pm 0.5^\circ\text{C}$ ) aqueous-phase cylindrical glass photoreactor (length: 9.5 cm, internal diameter: 6 cm) coupled with a thermostat (RCS, Lauda), were used to ensure constant temperature during irradiation. The solar simulator (LS0806, LOT-Quantum Design) consisted of a 1000 W Xenon lamp (LSB551LS0805, LOT-Quantum Design) coupled with an air mass filter (AM1-5G) that was positioned

160 20 cm away from the photoreactor (Fig. 2). This system has been designed to produce output power equivalent to 1 sun. Samples were thawed a few hours prior to irradiation and introduced into the photoreactor without any pre-filtration to maintain to natural composition of organic matterOM. Due to sampling volume limitations in the mesocosm, particularly for the SML,

available volumes for irradiation were 125 mL for ULW and 50 mL for the SML. To ensure the comparability of both experimental conditions, absorbed photon fluxes were estimated using ferrioxalate actinometry (Sect. 2.5).

165

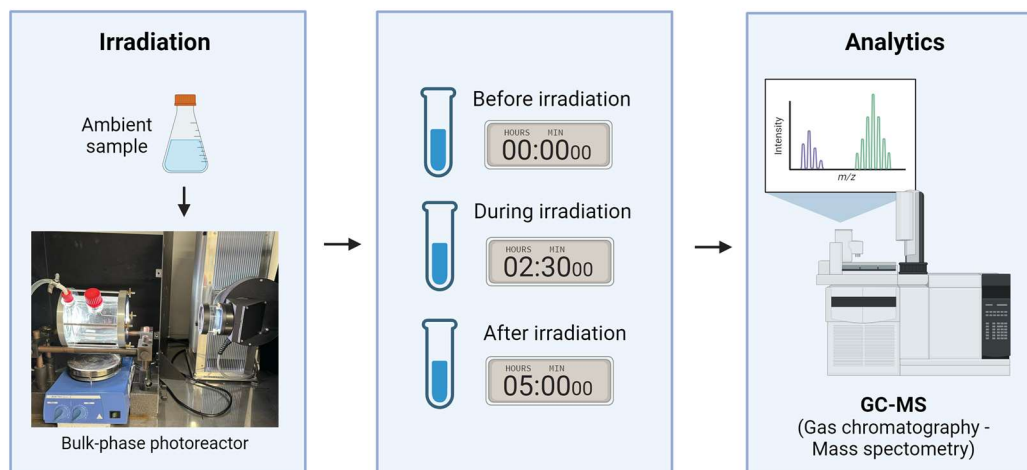


**Figure 2: Workflow for the analysis of photochemical production of carbonyl compounds in the SML and ULW samples. Seawater samples were irradiated for 5 hours, and aliquots of 10 mL were collected before the irradiation, after 2.5 hours and after 5 hours. The aliquots were filtered, derivatized with *o*-(2,3,4,5,6-pentafluorobenzyl)hydroxylamine (PFBHA), extracted with iso-octane and analyzed by GC-MS. Figure created with BioRender.com.**

170

During irradiation, all samples were continuously stirred with a magnetic stir bar and a magnetic stirrer (IKA RAH basic 2, IKA) to maintain homogeneous mixing and consistent light exposure. Aliquots of 10 mL were collected at three time points: (1) before irradiation, (2) after 2.5 hours, and (3) after 5 hours of irradiation. For the ULW samples, two to three replicates were collected at each time point, and the final reported concentrations represent the average. Due to the limited sample volumes of SML (50 mL per irradiation), replicates of the SML samples could not be taken.

175

After the 5 hours of irradiation, all the collected aliquots were either immediately processed together for the GC-MS analysis (Sect. 2.3), or stored at -20°C for later electron paramagnetic resonance (EPR) analysis (Sect. 2.4) and trace metal analysis (Sect. 2.6).

### 2.3 Analytical method for the quantification of carbonyl compounds

180

The analysis of the target carbonyl compounds was carried out using a method based on derivatization with a *o*-(2,3,4,5,6-pentafluorobenzyl)hydroxylamine (PFBHA) reagent (> 99 %, Sigma Aldrich), followed by solvent extraction and gas chromatography-mass spectrometry analysis (GC-MS; Agilent 8890 GC coupled to Agilent 5977C GC/MSD, Agilent Technologies) in selected ion monitoring (SIM) mode. The GC was equipped with a HP-5MS column (30 m × 250 μm × 0.25 μm, Agilent Technologies). This method was originally developed for marine samples by van Pinxteren and Herrmann (2013), and further optimized by Rodigast et al. (2015) for application to other environmental samples (Rodigast et al., 2015; van Pinxteren and Herrmann, 2013).

185

Ultra-pure water (resistivity > 18 MΩ.cm) was used for the preparation of all the solutions described in Sect. 2.3, 2.4, 2.5 and 2.6, and for the cleaning of all the laboratory glassware. Process blanks were prepared for each seawater sample by dissolving synthetic sea salts (Sigma Aldrich) in ultra-pure water at salinities depending on values reported by Bibi et al. and shown in Table 1 (Bibi et al., 2025). After irradiation, 8 mL of the seawater samples from the 10 mL aliquots and the corresponding blanks were filtered using sterile 10 mL plastic syringes (Braun) and 0.2 μm PTFE membrane syringe filters (Pall). As internal standard, 100 μL of a 4.21 μg L<sup>-1</sup> 2-(trifluoromethyl)benzaldehyde solution (98 %, Sigma Aldrich) prepared in ultra-pure water was added to each filtered sample. Afterwards, the derivatization solution was prepared by dissolving 30 mg of PFBHA (> 99 %, Sigma Aldrich) in 6 mL of ultra-pure water, and 200 μL were added to each of the samples. Then, 100 μL of hydrochloric acid (HCl) (37 %, CHEMSOLUTE) was added to accelerate the oxime formation. The prepared samples were allowed to react at room temperature for 18 hours in the dark to guarantee that the derivatization process was completed, and that the oximes of the carbonyl compounds are formed.

After the 18 hours of derivatization, iso-octane (> 99.5 %, Honeywell) was added as the extraction solvent (250 – 750 μL, depending on the expected DOM load of each sample), followed by 20 μL of HCl (37 %) to enhance the extraction efficiency. Samples were then mixed manually for one minute and shaken with an orbital shaker (IKA VIBRAX VXR basic, IKA) at 1000 rpm for 30 minutes. From the resulting organic phase formed in the upper part of the mixture, 100 μL of the iso-octane layer was separated and placed into an insert in a GC autosampler amber vial (Agilent Technologies), and covered with a 9 mm PTFE screw (Agilent Technologies). Five μL of the extract were injected into the GC-MS system in pulsed splitless mode. The initial temperature of the oven was 50°C, which was ramped to 210°C.

The calibration was performed in duplicates using seven concentration levels (between 10 and 200000 ng L<sup>-1</sup>), of standard carbonyl compounds, which were derivatized and extracted following the same procedure explained above for seawater samples.

Quantification was performed by normalizing the peak areas of all the carbonyl compounds to the peak area of the internal standard. Data were acquired using Agilent Enhanced MassHunter software, and a chromatographic analysis was performed using Agilent MassHunter Qualitative Analysis 10.0 and Agilent MassHunter Quantitative Analysis (for GCMS and LCMS). Relative compound-specific contributions were calculated from the quantified concentrations of each carbonyl compound relative to the total carbonyl concentration in each sample.

#### 2.4 Analytical method for the estimation of the photooxidation capacity

The in situ spin-probing experiments were performed in a Bruker EMX Plus spectrometer in a 4103TM resonator. The resonator was coupled with an optical fiber accessory preceded by a 1.0 mm SCHOTT WG280 filter irradiated with a 150 W Xenon arc lamp (Hamamatsu Photonics). Samples were introduced in the resonator in glass capillaries with a wavelength cut-off at the UVC range (below 280 nm). The EPR spectrometer settings were the following: microwave frequency = 9.853 GHz, modulation amplitude = 1.00 G, magnetic field scan = 150 G, sweep time = 15 s, conversion time = 10 ms, time constant = 5 ms, and two accumulations. Spectra were acquired in the field delay mode at a 1 s scan delay. SML and ULW samples

220 were added with the spin probe 1-hydroxy-3-methoxycarbonyl-2,2,5,5-tetramethyl pyrrolidine (CMH) (99 %, Noxygen), daily prepared at 10 mM in de-aerated ultra-pure water. Samples were added with 1 mM CMH, transferred to a 50  $\mu$ L capillary tube, centered in the resonator, and subsequently irradiated for 30 minutes. The pH of the samples was not modified during the analysis and was kept as  $8.4 \pm 0.1$ . A  $\text{Cr}^{3+}$  signal-intensity marker ( $g = 1.98$ , Bruker) was simultaneously measured with all samples. The simulation of the spectra and radical quantification were performed in the SpinCount software package available  
225 in Xenon (Bruker Corporation). The accuracy of the calibration was confirmed using the signal of 2,2,6,6-tetramethyl-1-piperidinyloxy (TEMPO) (99 %, Sigma-Aldrich). During the EPR measurements, it was confirmed that the resonator temperature remained stable at 298 K throughout the irradiation. The irradiation in the EPR was made using a 100 W Xenon lamp with radiation filters coupled to the resonator through an optical fibre, ensuring minimum transfer of infrared radiation and preventing sample heating.

230 Initially, SML and ULW samples were irradiated in the presence of 5,5-dimethyl-pyrroline N-oxide (DMPO), but no signals were observed over 30 minutes of irradiation, considering a limit of quantification of 100 nM. The samples were further irradiated in the presence of CMH. The CMH probe is known as an  $\text{O}_2^-$  radical probe due to its higher rate constant with these species ( $1.2 \times 10^4 \text{ M}^{-1} \text{ s}^{-1}$ ) when compared to other commonly used spin-trapping agents ( $k(\text{DMPO} + \text{O}_2^-) = 0.8 - 50 \text{ M}^{-1} \text{ s}^{-1}$ ). However, CMH also reacts with other reactive oxygen species (ROS) and one-electron oxidants, with rate constants of similar  
235 orders of magnitude (Gotham et al., 2020). The CMH autoxidation is also possible in the presence of CMH-reducible oxidants, such as metal ions, and it is therefore recommended that stock solutions are prepared in the presence of metal chelating agents. However, because the presence of complexing agents in seawater samples would affect their behaviour in photochemical experiments, daily stocks of CMH were prepared and a blank in ultra-pure water was measured before each analysis. The oxidation of CMH produced a nitroxide radical (here represented by CM radical) with a characteristic triplet EPR signal  
240 resulting from the hyperfine coupling between the unpaired electron of the CMnitroxide-radical and the nitrogen nucleus (aN).

Given the high lability of CMH, several precautions were taken to ensure the accuracy of the results. Several blanks were conducted to exclude the CMH autoxidation from the results observed in the presence of the irradiated SML samples. The rate of CMH autoxidation was subtracted from the rate of CM radical formation in the non-irradiated samples. This value was then  
245 normalized to the intensity of a  $\text{Cr}^{3+}$  marker signal ( $g = 1.98$ , Bruker) to guarantee signal homogeneity amongst experiments conducted over different days. We also observed small CM radical signals coming from the autoxidation of the stock solution of CMH prepared in ultra-pure water, which had minor contributions to the overall increase in the CM radical formation coming from the photoactivity of SML samples. Fig. S1 in the Supplementary Information illustrates the setup of the in situ EPR experiments.

## 250 2.5 Photon flux determination

As described in Sect. 2.3 and Sect. 2.4, two different setups were used for the photochemistry experiments. The absorbed photon fluxes in both experiments were determined using chemical actinometers, which are systems that contain a

chromophore with well-characterized quantum yield. Photon fluxes were quantified by monitoring of the light-induced formation or degradation of the photolysis product of the chromophore (Rabani et al., 2021; Kuhn et al., 2004). In order to  
255 normalize the photon flux in each system and ensure comparability of the obtained results, photon fluxes were estimated for the photoreactor ( $I_{PR}$ ) and for the capillary ( $I_{EPR}$ ).

#### *Photon flux in the photoreactor ( $I_{PR}$ )*

To estimate the photon flux in the photoreactor ( $I_{PR}$ ), the well-established potassium ferrioxalate actinometer developed by Hatchard and Parker was used (Hatchard and Parker, 1956). The potassium ferrioxalate solution ( $6 \times 10^{-3}$  M) was prepared  
260 following the detailed protocol described by Rabani et al., using ferric sulphate monohydrate (97 %, Sigma Aldrich), potassium oxalate monohydrate (99.98 %, Sigma Aldrich) and sulphuric acid (95 %, Fluka) (Rabani et al., 2021). As this actinometer is highly photosensitive and absorbs broadly between 200 to 600 nm, the preparation of the potassium ferrioxalate solution and the irradiation experiments were performed in a dark room only illuminated by red safety lamps. To represent the experimental conditions of both irradiated sample volumes (SML and ULW) described in Sect. 2.3, the actinometry experiments were  
265 performed with two solution volumes: 50 mL and 125 mL. A detailed explanation of the experimental procedure and the steps for the estimation of the photon fluxes are provided in Sect. S1 the Supplementary Information. The determined photon fluxes were  $2.7 \mu\text{mol of photons L}^{-1} \text{ s}^{-1}$  for 50 mL, and  $2.8 \mu\text{mol of photons L}^{-1} \text{ s}^{-1}$  for 125 mL.

#### *Photon flux in the capillary ( $I_{EPR}$ )*

270 The photon flux in the capillary for the EPR experiments ( $I_{EPR}$ ) was determined using the method proposed by Moan et al. (1979) with the generation of <sup>1</sup>O<sub>2</sub> singlet oxygen from the irradiation of a porphyrin solution (Protoporphyrin IX – Target Mol) in the presence of 2,2,6,6-tetramethyl-4-piperidinol (TEMPOL) (98 %, Sigma-Aldrich) (Moan et al., 1979). This method was further optimized for its implementation to ambient seawater samples ((Scheres Firak et al., in press) ~~Scheres Firak et al., in preparation~~). The quantum yield for the production of singlet oxygen  $\phi(^1\text{O}_2)$  by Protoporphyrin IX is 0.77 (Nishimura et al.,  
275 2020). The photon flux for the in situ EPR experiments was estimated as  $(9 \pm 2) \times 10^{-9}$  mol photons  $\text{L}^{-1} \text{ s}^{-1}$  using the irradiation of Protoporphyrin IX solution ( $c_0 = 10 \mu\text{M}$ ) in the presence of TEMPOL ( $c_0 = 100 \mu\text{M}$ ).

## **2.6 Analytical method for the measurement of trace metals**

Trace concentrations of iron (Fe) and copper (Cu) were measured directly from the seawater samples using a benchtop total reflection X-ray fluorescence (TXRF) S4 T-STAR spectrometer (Bruker AXS). Five  $\mu\text{L}$  of seawater sample were spiked with  
280 5 ng (50 ng for samples collected on June 11<sup>th</sup>) internal standard of Sc/Co in ultra-pure water solution, on a TXRF quartz carrier. Before the measurement, the TXRF carriers were allowed to dry at  $80^\circ\text{C}$  on a hot plate for about 5 minutes. Each analysis lasted typically 500 s. X-ray data acquisition and quantification of elemental concentrations was performed using the SPECTRA 6.2 software. This method was originally developed by Fomba et al. for the investigation of trace metal concentrations in particulate matter (PM) and cloud water (Fomba et al., 2013; Fomba et al., 2020), and further optimized for

285 its application to seawater samples in the present study. To represent the three stages of the phytoplankton bloom, we analyzed the SML and ULW samples collected on May 20<sup>th</sup> (pre-bloom) and June 2<sup>nd</sup> (bloom).

## 2.7 Text management

ChatGPT (Open AI, 2025) was used for language polishing assistance.

## 3 Results and discussion

### 290 3.1 Concentrations of carbonyl compounds in irradiated samples under bloom and non-bloom conditions

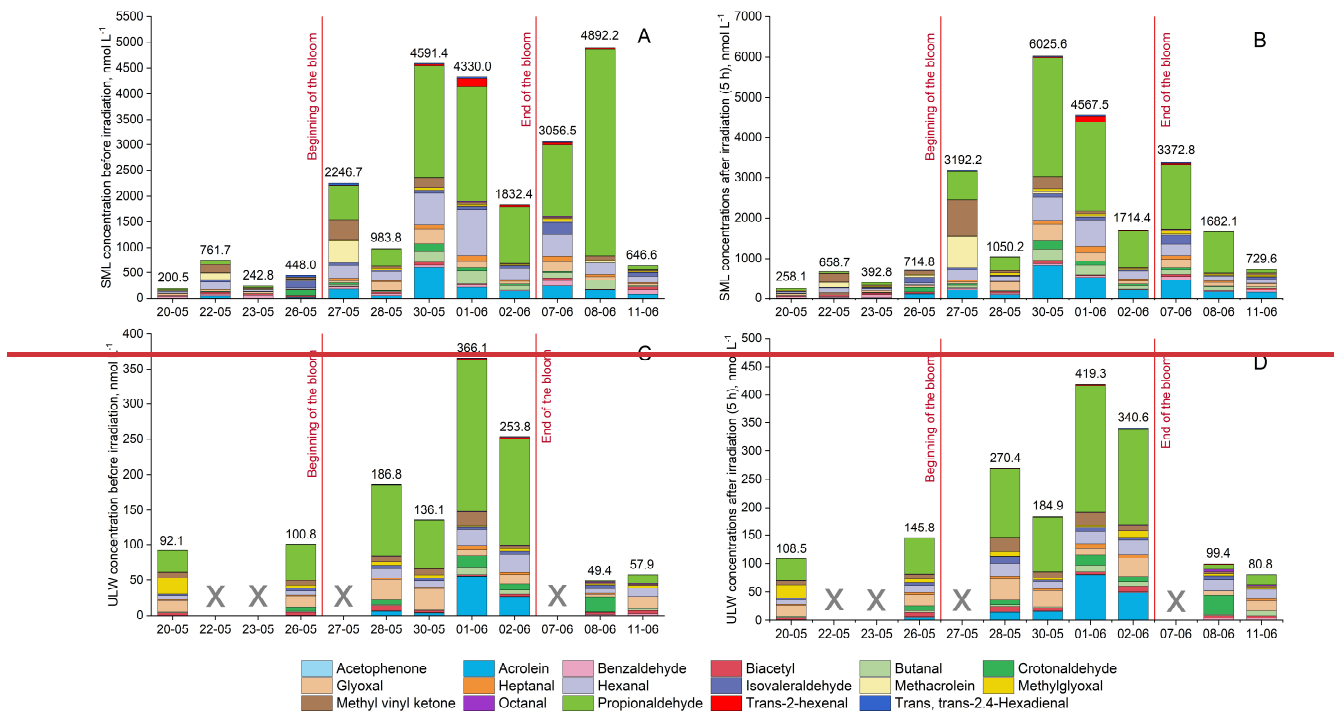
Figure 3 illustrates the individual concentrations in the seawater samples of the 17 carbonyl compounds in four categories: SML before irradiation (A), SML after 5 hours of irradiation (B), ULW before irradiation (C), and ULW after 5 hours of irradiation (D). Relative changes induced by irradiation (% increase/decrease) in carbonyl compound concentrations are shown in Figure S3 (Supplementary Information) to facilitate comparison of photochemical responses across compounds. The observed photochemical transformations of carbonyl compounds likely arise from the combined processing of both the DOM and POM (including intact cells, cellular debris, and particulate biological material potentially released during freeze-thaw cycles). As a result, the reported photochemical rates represent the integrated responses of the total OM pool present in the SML and in ULW.

Carbonyl concentrations varied considerably between SML and ULW, and across bloom phases. Total carbonyl concentrations were generally higher in samples collected during the bloom phase compared to the pre- and post-bloom phases, with exception of the SML sample collected on June 8<sup>th</sup> (A). In that day, the concentration of propanal before irradiation reached 4027 nmol L<sup>-1</sup>, a value significantly higher than in the irradiated counterpart (B). Propanal and hexanal were the most abundant compounds during the bloom phase, suggesting that their formation is favoured under conditions of high biological productivity. Propanal exhibited remarkably higher concentrations with respect to other species, particularly in the SML during the bloom and post-bloom phases. This suggests that propanal may represent an important, yet previously underrecognized, contributor to the carbonyl pool at the air-sea interface. Further targeted studies with increased temporal resolution and replication are required to better understand the specific mechanisms driving its massive production in these conditions.

Throughout all bloom phases, the SML (A and B) had consistently higher concentrations than the ULW samples (C and D) both before and after irradiation, despite similar photon fluxes were confirmed by actinometry (see Sect. 2.5). Before irradiation, values in the SML (A) ranged from 201 to 762 nmol L<sup>-1</sup> in the pre-bloom phase, 984 to 4591 nmol L<sup>-1</sup> in the bloom phase, and 647 to 4894 nmol L<sup>-1</sup> in the post-bloom phase; while in the ULW (C) they were significantly lower (e.g., 136 to 366 nmol L<sup>-1</sup> in the bloom phase). After 5 hours of irradiation, the concentrations of carbonyl compounds increased further, reaching up to 6026 nmol L<sup>-1</sup> in the SML (B) during the bloom phase and 419 nmol L<sup>-1</sup> in the ULW (D). This suggests the light-driven production of aldehydes and ketones, probably via direct photolysis, photochemical oxidation or photosensitized reactions. These observed SML enrichments for all the aldehydes and ketones under evaluation are in agreement with previous

studies for glyoxal, methylglyoxal, propanal and butanal (Zhou and Mopper, 1997; van Pinxteren and Herrmann, 2013), and provide novel insights on the behaviour of a larger pool of carbonyl compounds with potential relevance in the marine environment, such as MVK or methacrolein. Overall, our findings indicate that the unique physical and chemical environment in the surface of the sea, richer in organic compounds compared to ULW, favours the production of these carbonyl compounds.

320 These trends could be attributed to several factors, such as the diverse chemical composition, reactivity, optical properties and availability of the DOM in the different water layers. Surface waters are typically characterized by their enrichment in more photoreactive and autochthonous DOM, contrasting with the more degraded and refractory compounds in the underlying waters (Wagner et al., 2020; Yang et al., 2022).



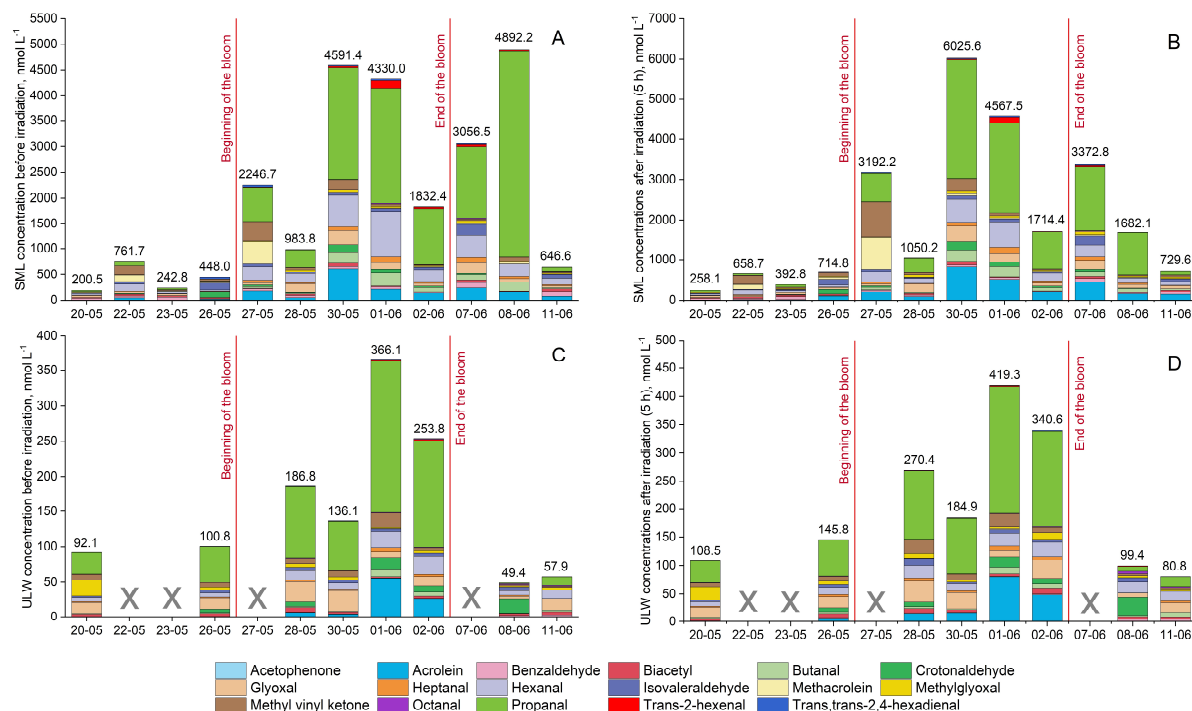


**Figure 3: Speciation of 17 carbonyl compounds in SML samples before irradiation (A) and after 5 hours of irradiation (B), and ULW samples before irradiation (C) or after irradiation (D). The red lines separate the three phases of the mesocosm experiment. ULW samples collected on May 22<sup>nd</sup>, May 23<sup>rd</sup>, May 27<sup>th</sup> and June 7<sup>th</sup> were not available for their analysis.**

325

330 Our data shows higher concentrations of carbonyl compounds generally during the phytoplankton bloom phase (Fig. 3), suggesting a strong direct or indirect influence of biological productivity on the availability of precursors for the production of aldehydes and ketones. Higher concentrations were partly found in the post-bloom compared to the pre-bloom. This pattern is in agreement with the parallel increase of the DOC levels with the phytoplankton abundance in the bloom phase, and with how these levels also remained high in the post-bloom phase (Fig. 1). Generally, high variability in the concentrations of

335 humic-like compounds and in the ratios of labile/refractory compounds were found through the duration of the mesocosm, which supports the idea of bloom-dependent DOM transformations ((Thölen et al., 2026; Zöbelein et al., 2026)Thölen et al., in preparation; Zöbelein et al., in preparation). Fresh biological material produced during phytoplankton blooms is a source of photochemically-active DOM. For instance, *Emiliana huxleyi*, a specie of photosynthetic coccolithophore that dominated at the early bloom phase (Bibi et al., 2025), is characterized by its efficient photochemical production of isoprene, a volatile

340 precursor of several carbonyl compounds (Shaw et al., 2003; Sinha et al., 2007). Comparable trends have been observed in marine diatoms and dinoflagellates (Moore et al., 1994; Milne et al., 1995), which may explain the formation of carbonyl compounds in marine environments. For instanceLikewise, the photochemical production of aldehydes and ketones from lipids

derived from *Chaetocerus pseudocurvisetus* has been recently demonstrated (Penezic et al., 2023). Furthermore, the major fatty acids from other diatoms like *Phaeodactylum triconutum* might be precursors of hexanal through oxidation reactions (Schobert and Elstner, 1980). Oxidative stress during blooms and photochemical degradation of DOM are linked to the massive production of ROS (Hansel and Diaz, 2021), which may trigger processes like isoprene oxidation and lipid peroxidation, leading to the release of aldehydes and ketones.

Altogether, this experimental evidence indicates that phytoplankton blooms influence not only the biological activity in seawater but may also modulate abiotic processes, particularly in the SML, by changing DOM chemical composition and reactivity.

### 3.2 Photochemical production rates under bloom and non-bloom conditions

We investigated the photochemical formation and degradation rates of the 17 carbonyl compounds, expressed in  $\text{nM h}^{-1}$ , in both SML and ULW samples (Fig. 4 and Fig. 5, expressed in  $\text{mol mol(DOC)}^{-1} \text{h}^{-1}$ ). In the three phases of the mesocosm study, the carbonyl compounds in the SML samples (red) presented consistently higher photochemical production rates than in the ULW (blue). These findings are likely due to the enrichment of photochemically-active compounds and surface-active molecules, such as lipids, fatty acids and aromatic compounds in the SML; which contrast with the more processed and aged DOM typically present in the ULW (Sect. 3.1).

The photochemical production rates in the SML and ULW of the 17 carbonyl compounds were classified in two major categories, based on how their time-resolved photochemistry was influenced by the phytoplankton bloom:

#### *Photochemistry influenced by the bloom*

Ten out of 17 compounds showed enhanced photochemical formation or degradation in the SML during the phytoplankton bloom: MVK, methacrolein, glyoxal, methylglyoxal, acrolein, crotonaldehyde, heptanal, biacetyl, hexanal and trans-2-hexenal.

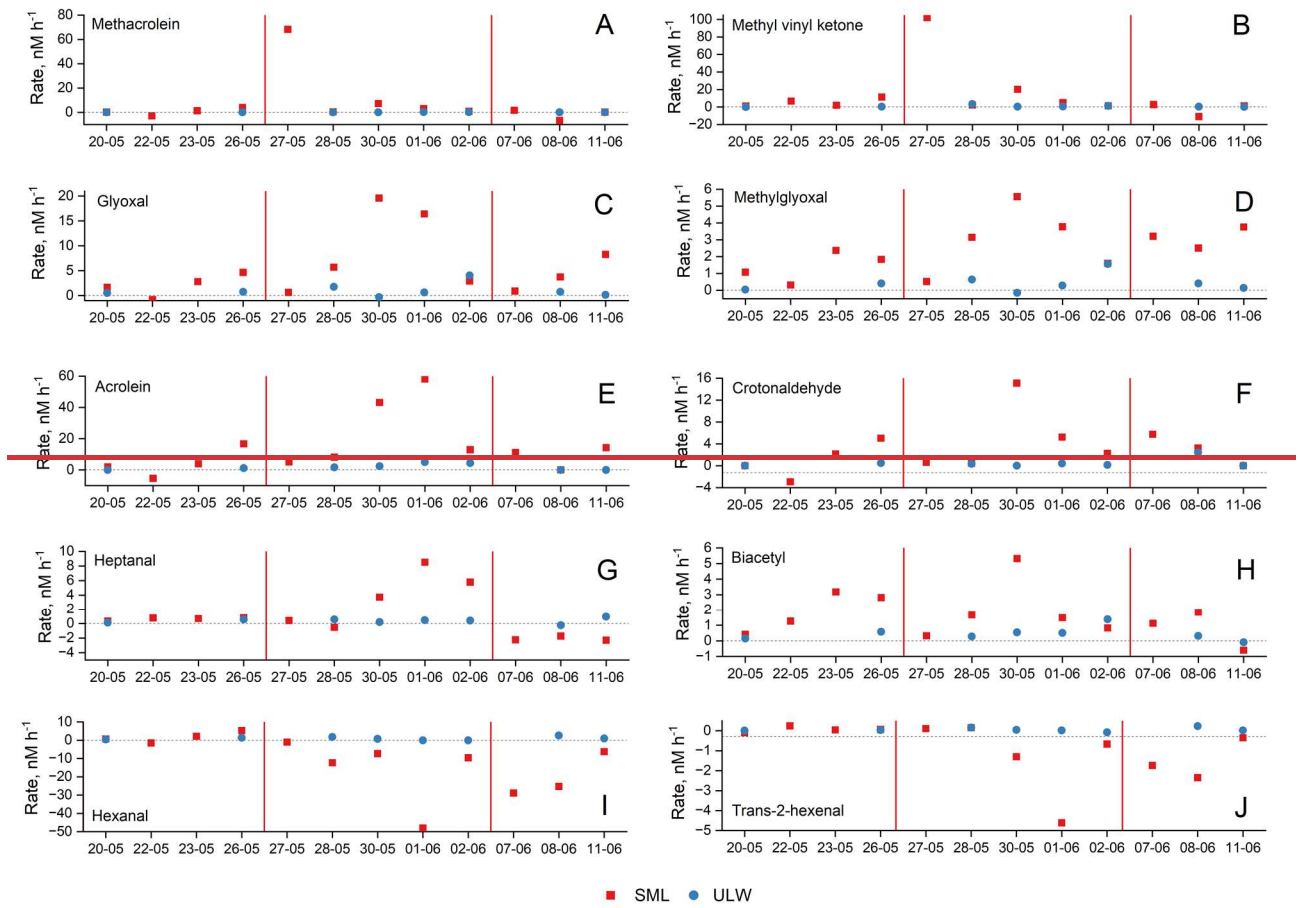
These trends suggest an influence of the stage of the phytoplankton bloom in the photochemical activity of these 10 carbonyl compounds in the SML, presumably due to the elevated concentrations of photochemically-active precursors and higher oxidative stress. Even though the overall DOC concentrations remained relatively stable during the bloom and post-bloom phases of the mesocosm study (Fig. 1), the fresher and more photoreactive nature of the phytoplankton-derived CDOM and photosensitizers in the bloom phase seemed to enhance the generation of excited triplet-state DOM and ROS, promoting the photochemical production of these carbonyl compounds in the SML.

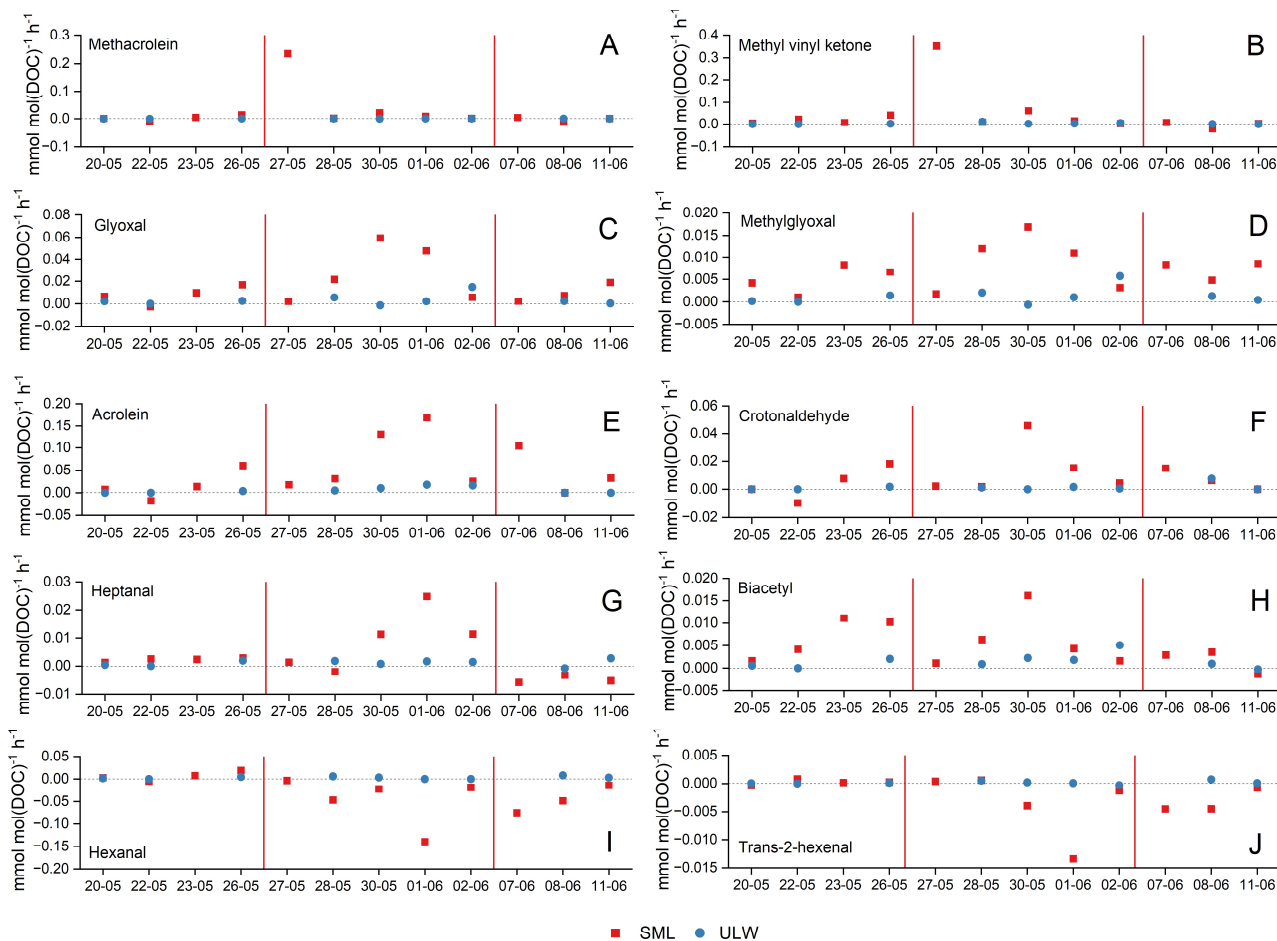
Interestingly, the temporal behaviour of the production rates of isoprene oxidation products had a characteristic pattern: methacrolein (A) and MVK (B), both primary isoprene products, had peak productions in the early stage of the bloom; while glyoxal (C), methylglyoxal (D) and acrolein (E), all secondary isoprene products, dominated the later stage of the bloom. This temporal pattern suggests a dynamic photochemical response in the SML regarding isoprene formation likely driven by the changes in the composition of DOM throughout a phytoplankton bloom. Isoprene is a trace gas produced both photochemically

at the sea surface (Wang et al., 2023) and biologically by marine phytoplankton (Moore et al., 1994; Simó et al., 2022; Sinha et al., 2007; Ciuraru et al., 2015). In seawater, it is typically present in concentrations of few pmol L<sup>-1</sup> (Conte et al., 2020; Milne et al., 1995). In the atmosphere, isoprene can undergo an oxidation reaction, for example, with OH radicals, NO<sub>3</sub> radicals or O<sub>3</sub> (Atkinson, 2000), yielding MVK and methacrolein as primary products, and acrolein, glyoxal and methylglyoxal as secondary products. Indeed, nearly 50 % of glyoxal and more than 70 % of methylglyoxal in the atmosphere are estimated to originate from isoprene oxidation (Fu et al., 2008). ~~Although these degradation pathways have been widely studied in the gas phase,~~ The aqueous-phase photooxidation of isoprene by OH radicals has also been demonstrated (Huang et al., 2011), and  
~~Due to the intense solar radiation and the presence of OH radicals in the SML (Zhou and Mopper, 1990a), isoprene-derived species such as MVK, methacrolein, acrolein, glyoxal and methylglyoxal are likely formed in this environmente-SML.~~  
Oxidation of acetone, glycolaldehyde and acetaldehyde also yields glyoxal and methylglyoxal (Walker et al., 2022); indeed, acetone has been reported to be responsible for more than 7 % of the global production of methylglyoxal (Fu et al., 2008). There is experimental evidence of marine production of acetaldehyde and acetone (de Bruyn et al., 2011; Kieber et al., 1990; Sinha et al., 2007; Zhu and Kieber, 2018; Millet et al., 2010; Wang et al., 2019; Mopper et al., 1991), and the unique environment of the SML could facilitate their transformation into other carbonyl compounds. Additionally,  
~~The formation of acrolein and glyoxal from the OH-driven oxidation or ozonolysis of hydrocarbons, such as 1,3-butadiene, benzene, toluene, acetylene and xylene, another diene monomer,~~ has been reported to yield carbonyl compounds like acrolein, glyoxal, methylglyoxal and biacetyl  
~~observed in the gas phase (Tuazon et al., 1999; Jaoui et al., 2025). Aromatic hydrocarbons, such as benzene, toluene, acetylene and xylene, also undergo OH-initiated oxidation in the atmosphere primarily through ring-cleavage, yielding glyoxal, methylglyoxal and biacetyl (Volkamer et al., 2001; Tuazon et al., 1986; Fu et al., 2008). These dicarbonyls can be either transferred to seawater via atmospheric deposition, or formed in situ.~~  
In summary, these well-characterized degradation pathways in the gas phase provide useful mechanistic analogues for understanding possible photochemical transformations of these compounds in the SML.  
Phytoplankton and algae produce polyunsaturated fatty acids (PUFAs) and saturated fatty acids, which degrade via reactions with radicals and lead to the formation of carbonyl compounds. Peroxidation of lipids is a source of a diverse pool of carbonyl compounds including acrolein, butanal, crotonaldehyde, glyoxal, hexanal, propanal, and trans-2-hexenal (Uchida et al., 1998; Zhou et al., 2014; Onyango, 2012; Kato et al., 2022; Wu and Lin, 1995). For instance, the enzymatic breakdown of linoleic acid by lipoxygenase and hydroperoxide lyase in marine algae yields hexanal (Boonprab et al., 2003). In addition to that, trans,trans-2,4-hexadienal may also form as an oxidation product of fatty acids (Ferrario et al., 1985).  
Enhanced photochemical degradation of hexanal (I) and trans-2-hexenal (J) was also observed during the bloom phase. Both  
~~compounds presented the highest photochemical degradation rates on June 1<sup>st</sup>, -0.14,48.0 μmol mol(DOC)<sup>-1</sup>M h<sup>-1</sup> for hexanal and -0.014,6 μmol mol(DOC)<sup>-1</sup>nM h<sup>-1</sup> for trans-2-hexenal. This coincides with the expected generation of large quantities of ROS, such as OH radicals, O<sub>2</sub><sup>-</sup>superoxide and <sup>1</sup>O<sub>2</sub> singlet oxygen linked to oxidative stress in phytoplankton blooms (Cho et al., 2022). These species would be massively available during the bloom to degrade hexanal and trans-2-hexenal, a process similar to what has been observed in the gas phase (Jiménez et al., 2007; Tadic et al., 2001).~~

410 Phytoplankton and algae produce polyunsaturated fatty acids (PUFAs) and saturated fatty acids, which degrade via reactions  
with radicals and lead to the formation of carbonyl compounds. Peroxidation of lipids is a source of a diverse pool of carbonyl  
compounds including acrolein, butanal, crotonaldehyde, glyoxal, hexanal, propanal, and trans-2-hexenal (~~!!! INVALID  
CITATION !!!~~ (Uchida et al., 1998; Zhou et al., 2014; Onyango, 2012; Kato et al., 2022; Wu and Lin, 1995)). For instance,  
415 the enzymatic breakdown of linoleic acid by lipoxygenase and hydroperoxide lyase in marine algae yields hexanal (Boonprab  
et al., 2003). In addition to that, trans,trans-2,4-hexadienal may also form as an oxidation product of fatty acids (Ferrario et al.,  
1985).

In general, carbonyl compounds can be degraded by undergo photolysis and radical-driven oxidation (Atkinson, 2000; Epstein  
et al., 2013; Tilgner and Herrmann, 2010), processes that are likely intensified by the high concentrations of DOM and strong  
solar radiation characteristic of the SML. ~~One of the dominant removal processes of aldehydes in the atmosphere is photolysis  
420 (!!! INVALID CITATION !!! (Atkinson, 2000)), and analogous mechanisms are also expected to occur in the marine boundary  
layer.~~ In the gas phase, photolysis and oxidation by OH radicals have been estimated to account for up to 76 % of glyoxal and  
82 % of methylglyoxal removal (Fu et al., 2008). Likewise, tropospheric losses of hexanal and trans-2-hexenal are also mainly  
attributed to reactions with OH radicals (Jiménez et al., 2007). OH radicals react with aldehydes and ketones via hydrogen  
abstraction from the -CHO group (Atkinson, 2000), and as these. OH radicals are continuously formed in seawater via  
425 photochemical reactions involving CDOM (Zhou and Mopper, 1990a), ~~suggesting that~~ OH-oxidation is a significant sink of  
carbonyl compounds in the SML. Ozone can be highly reactive towards marine DOC, potentially contributing to the production  
of VOCs in seawater, such as glyoxal, propanal, hexanal, heptanal and octanal (!!! INVALID CITATION !!! (Wang et al.,  
2023; Kilgour et al., 2024; Carpenter and Nightingale, 2015)). For instance, the formation of hexanal via ozonolysis of  
unsaturated fatty acids has been widely demonstrated (!!! INVALID CITATION !!! (Zhou et al., 2014; Moise and Rudich,  
430 2002; Thornberry and Abbatt, 2004)). Given that the large pool of available DOC with its unsaturated fraction could become  
reaction partners to ozone from the gas phase, these formation pathways are potentially of high relevance.



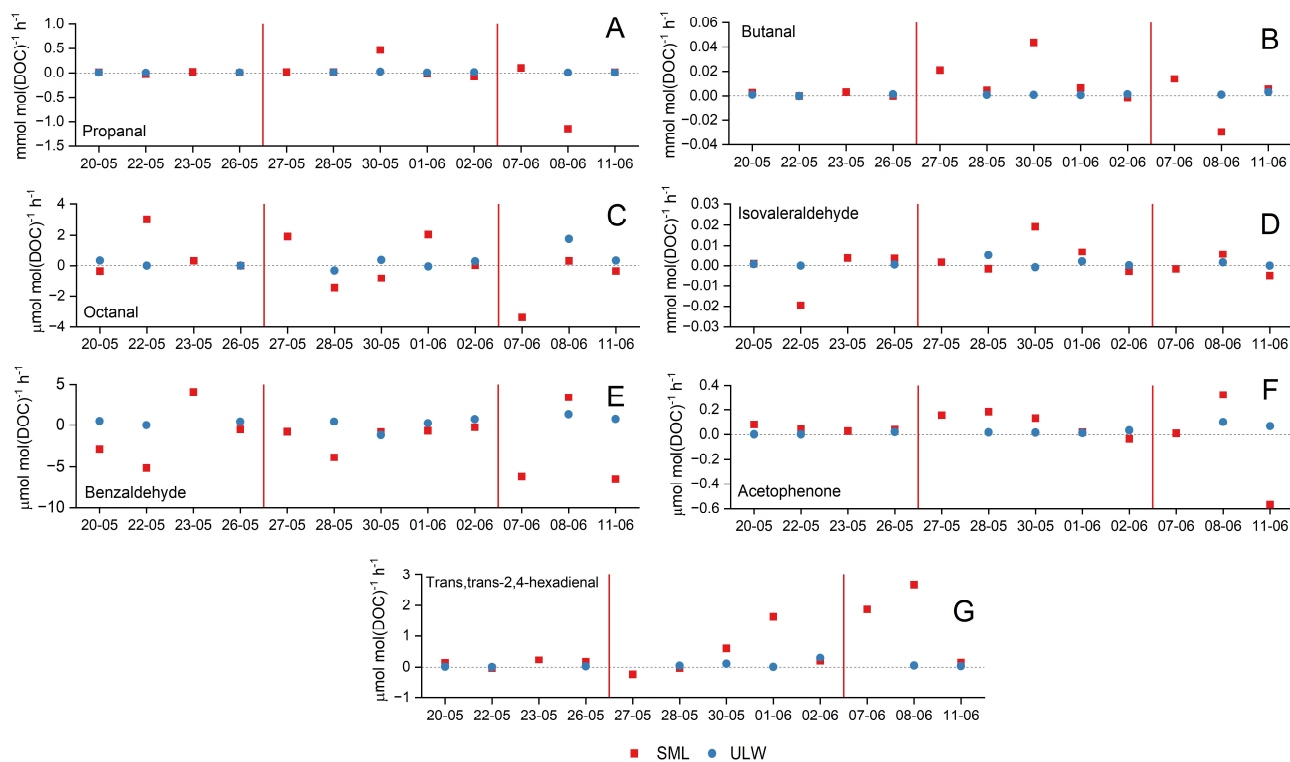


435 **Figure 4: Comparison of photochemical formation and degradation rates of methacrolein (A), MVK (B), glyoxal (C), methylglyoxal (D), acrolein (E), crotonaldehyde (F), heptanal (G), biacetyl (H), hexanal (I) and trans-2-hexenal (J) in the SML (red) and in ULW (blue). The red vertical lines separate the three phases of the mesocosm study: pre-bloom (20-05 to 26-05), bloom (27-05 to 02-06) and post-bloom (08-06 to 11-06). Photochemical production and degradation rates in the ULW samples on an expanded scale, including error bars that reflect analytical and sample-handling uncertainties, are shown Figure S4 in the Supplementary Information.**

440

445 ~~These trends suggest an influence of the stage of the phytoplankton bloom in the photochemical activity of 10 carbonyl compounds in the SML, presumably due to the elevated concentrations of photochemically active precursors and higher oxidative stress. Even though the overall DOC concentrations remained relatively stable during the bloom and post-bloom phases of the mesocosm study (Fig. 1), the fresher and more photoreactive nature of the phytoplankton-derived CDOM and photosensitizers in the bloom phase seemed to enhance the generation of excited triplet-state DOM and ROS, promoting the photochemical production of these carbonyl compounds in the SML.~~





455

**Figure 5: Comparison of photochemical formation and degradation rates of propanal (A), butanal (B), octanal (C), isovaleraldehyde (D), benzaldehyde (E), acetophenone (F) and trans,trans-2,4-hexadienal (G) in the SML (red) and in ULW (blue). The red lines separate the three phases of the mesocosm study: pre-bloom (20-05 to 26-05), bloom (27-05 to 02-06) and post-bloom (08-06 to 11-06). Photochemical production and degradation rates in the ULW samples on an expanded scale, including error bars that reflect analytical and sample-handling uncertainties, are shown Figure S4 in the Supplementary Information.**

460

Propanal (A) and butanal (B) were the most photochemically active compounds in this category. They are small aldehydes commonly linked to the oxidation of larger organic molecules, which could explain their abundance in the different phases of the study. The photochemical activity of the aromatic carbonyls, benzaldehyde (E) and acetophenone (F), peaked in the pre- and post-bloom phases and was relatively lower than for the other compounds. This could suggest an increased presence of humic-like DOM derived from anthropogenic activity or terrestrial sources, which is less labile but still photochemically active. The photooxidation of aromatic hydrocarbons can also lead to the production of aromatic carbonyls, such as acetophenone and benzaldehyde (Ehrhardt and Petrick, 1984; Ehrhardt et al., 1982). Aromatic hydrocarbons are generally considered anthropogenic, but marine phytoplankton has also been reported as a source particularly under oxidative stress (Rocco et al., 2021). In addition to aromatic hydrocarbons, the photodegradation of polystyrene nanoparticles by OH radicals or ozone generates acetophenone and benzaldehyde (Davidson et al., 2005; Bianco et al., 2020; Fabbri et al., 2023). The presence of these compounds in the seawater samples suggests plastic contamination, which in nature also contributes to the release of carbonyl compounds. However, the concentrations of acetophenone and benzaldehyde accounted only for up to 2

470

475 % of the total sum composition of carbonyl compounds in SML samples, so these sources appear to be minor. The production of octanal (C) and trans,trans-2,4-hexadienal (G) is also comparatively lower, likely because it requires the preservation of longer carbon chains and more complex structures.

480 In general, the high photochemical production rates observed in the later stage of the bloom and during the post-bloom phase of the experiment may be explained by the photochemical degradation of lipids and humic-like compounds as precursor molecules, which could represent a higher proportion of the DOM due to the beginning of the phytoplankton decay from viral cell lysis, senescence or grazing (Rochelle-Newall et al., 1999).

485 To facilitate comparison with existing literature, the non-normalized rates were also calculated and are provided in the Supplementary Information (Figure S8 and Figure S9). The findings for glyoxal and methylglyoxal in non-bloom phases are consistent with published photochemical production rates from SML samples collected in the Bahamas, Delaware Bay (USA) and Biscayne Bay (USA), which range between 0.75 and 5.8 nM h<sup>-1</sup> for glyoxal, and 0.3 and 2.5 nM h<sup>-1</sup> for methylglyoxal (Mopper and Stahovec, 1986; Zhou and Mopper, 1997). On the other hand, the higher photochemical formation rates found during the bloom phase for these two compounds were comparable with those reported by Zhou and Mopper for SML samples (up to 15.5 nM h<sup>-1</sup> for glyoxal and 9.7 nM h<sup>-1</sup> for methylglyoxal), collected in the Biscayne Bay in the presence of foam on the sea surface (Zhou and Mopper, 1997). Likewise, rates of photochemical formation reported in the ULW align well with those determined in the present study (Zhu and Kieber, 2018; Zhou and Mopper, 1997). Higher photochemical activity in short-chain aldehydes was observed, compared to literature values: Zhou and Mopper reported formation rates between 1.3 and 7.4 nM h<sup>-1</sup> for C<sub>3</sub> aldehydes, and between 0.4 to 4.2 nM h<sup>-1</sup> for C<sub>4</sub> aldehydes (Zhou and Mopper, 1997). Despite the lower magnitudes compared to the present study, Mopper and Stahovec also observed photochemical degradation of propanal (-0.75 nM h<sup>-1</sup>) in surface water samples from the Biscayne Bay (Mopper and Stahovec, 1986).

495 Apparent quantum yields (AQYs) were calculated from the measured photoproduction rates and the absorbed photon fluxes (Supplementary Information, Sect. S6). Because the experiments were conducted using unfiltered samples, the derived AQYs represent effective photochemical efficiencies of the total OM pool, including both DOM and POM. The results demonstrate that the SML is a more photochemically efficient environment compared to ULW, particularly during the bloom phase. No systematic relationship was observed between AQYs and DOC concentrations (Supplementary Information, Figure S5), suggesting that OM abundance alone does not control the efficiency of these photochemical processes.

500 By connecting phytoplankton bloom dynamics and the temporal trend of the photochemical products, our results stress the crucial role of the SML as a dynamic air-sea boundary and its potential implications for the production of VOCs to the marine atmosphere. These findings are of high relevance for refining atmospheric models in the marine environment, as climate change is projected to cause shifts in nutrient and sunlight availability, thereby influencing phytoplankton blooms and marine carbon cycling (Thomalla et al., 2023; Dai et al., 2023).

510 ~~The observed photochemistry of carbonyl compounds is shaped by multiple in situ processes that contribute to their formation and removal, so understanding potential sources and sinks of these compounds in the marine environment is essential for a better interpretation of our findings. These sources and sinks include chemical pathways, biological activity and anthropogenic inputs. In this section, key processes contributing to the production or loss of carbonyl compounds in the marine environment are discussed, with special focus on how they may be enhanced in the SML due to higher DOM concentrations and intense solar irradiation characteristic of the marine interface.~~

~~*Isoprene-derived oxidation products:*~~

~~*Secondary carbonyl compound formation from other carbonyl compounds:*~~

515 ~~*Fatty acid degradation:*~~

520 ~~*Reactions involving ozone (O<sub>3</sub>):* Ozone can be highly reactive towards marine DOC, potentially contributing to the production of VOCs in seawater, such as glyoxal, propanal, hexanal, heptanal and octanal (Wang et al., 2023; Kilgour et al., 2024; Carpenter and Nightingale, 2015). For instance, the formation of hexanal via ozonolysis of unsaturated fatty acids has been widely demonstrated (Zhou et al., 2014; Moise and Rudich, 2002; Thornberry and Abbatt, 2004). Given that the large pool of available DOC with its unsaturated fraction could become reaction partners to ozone from the gas phase, these formation pathways are potentially of high relevance.~~

525 ~~*Aromatic hydrocarbon oxidation:* Aromatic hydrocarbons such as benzene, toluene, acetylene and xylene undergo OH-initiated oxidation in the atmosphere primarily through ring cleavage, yielding glyoxal, methylglyoxal and biacetyl (Volkamer et al., 2001; Tuazon et al., 1986; Fu et al., 2008). These dicarbonyls can be either transferred to seawater via atmospheric deposition, or formed in situ. The photooxidation of aromatic hydrocarbons can also lead to the production of aromatic carbonyls, such as acetophenone and benzaldehyde (Ehrhardt and Petrick, 1984; Ehrhardt et al., 1982). Aromatic hydrocarbons are generally considered anthropogenic, but marine phytoplankton has also been reported as a source particularly under oxidative stress (Rocco et al., 2021).~~

530 ~~*Other anthropogenic sources:* In addition to aromatic hydrocarbons, the photodegradation of polystyrene nanoparticles by OH radicals or ozone generates acetophenone and benzaldehyde (Davidson et al., 2005; Bianco et al., 2020; Fabbri et al., 2023). The presence of these compounds in the seawater samples suggest plastic contamination, which in nature also contributes to the release of carbonyl compounds. However, the concentrations of acetophenone and benzaldehyde accounted only for up to 2 % of the total sum composition of carbonyl compounds in SML samples, so these sources appear to be minor.~~

535

~~*Photolysis and radical-driven oxidation of carbonyl compounds:*~~

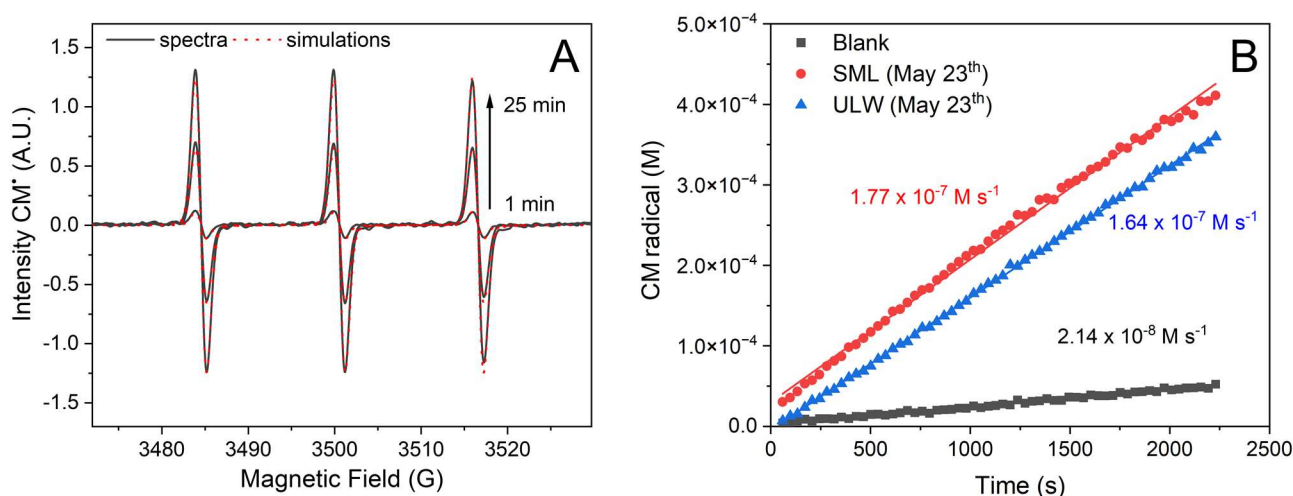
540 ~~*Air-sea exchanges:* Air-sea exchanges and wet deposition may act as a sources of carbonyl compounds in SML, either by their direct deposition or by introducing new precursors for aqueous phase processes (Zhou and Mopper, 1990b; Sinha et al., 2007). Finally, air-sea exchanges could also act as removal mechanisms of carbonyl compounds in seawater (Zhou and Mopper, 1990b; Sinha et al., 2007), particularly those of higher volatilities (more details in Sect. 3.4).~~

~~Several of the processes described above are widely documented in atmospheric systems, but experimental evidence for their occurrence in seawater remain limited. Nevertheless, the combination of high DOM concentrations and strong~~

~~solar radiation in the SML suggest that mechanisms such as lipid peroxidation or isoprene oxidation are probably dominant sources of carbonyl compounds in the marine boundary layer.~~

### 545 3.3 Photooxidation capacity under bloom and non-bloom conditions

Investigations of photooxidation capacity in the seawater samples are essential to understand how the sunlight-driven production of reactive intermediates influences the transformation of DOM and the subsequent formation of VOCs. The photooxidation capacity of SML and ULW samples was tested using a radical probe in EPR experiments. Since radicals are short-lived species, they require probes or spin-trapping agents that react with radicals to form stable paramagnetic species that can be further detected with an EPR spectrometer. Nitroxides such as 5,5-dimethyl-pyrroline N-oxide (DMPO) and 1-hydroxy-3-methoxycarbonyl-2,2,5,5-tetramethyl pyrrolidine (CMH) are respective examples of spin-trapping agents and spin probes typically used to investigate the formation of radicals in ambient samples (Briedé et al., 2005; Arangio et al., 2016). As seen in Fig. 6, the formation of CM radicals occurred in all samples and increased linearly during the monitored time. These values were then represented in bar plots that illustrate the overall budget of oxidants photochemically generated in the samples (Fig. 7).



560 **Figure 6: (A) EPR spectra of CM radicals at different irradiation times. Spectral parameters:  $a_N = 16$  G,  $g = 2.0056$ . (B) Profile of CM radical formation over time for blank, SML, and ULW samples. The blank in (B) represents the CM radical formation in the absence of light. The resultant signals were subsequently plotted as a function of the irradiation time, and fitted to a linear regression to get the rate of CM radical formation over time. The formation of CM radical was normalized by the ratio between  $I_{EPR}$  and  $I_{PR}$ . This normalization procedure yields CM radical formation rates that account for the energy input of the photoreactor, which is circa 300 times greater than the energy input in the in situ EPR experiments due to the smaller sample volumes required for the EPR measurements.**

565

As presented in Fig. 7, the overall photochemical oxidation capacity of the samples did not seem to be affected by the addition of nutrients. It was also, on average, similar for both SML and ULW samples, with values around  $34 \mu\text{M s}^{-1}$ . To evaluate whether these results reflect enhanced photochemical reactivity or simply the highest abundance of OM the measured

photooxidation capacities were compared to DOC concentrations (Supplementary Information, Figure S7). No systematic correlation was found, indicating that the observed results cannot be explained solely by the abundance of OM.

While nutrient levels can indirectly influence the redox capacity of seawater samples through phytoplankton blooms, they ultimately did not appear to control it. The oxidation potential of the samples seemed to be primarily determined by the presence and availability of electron donors and acceptors. Although the complexity of the mesocosm samples makes it difficult to attribute the oxidation properties to individual species, a dominant class of redox-active compounds known to be present in seawater are metal ions. Nutrient levels, while impacting the concentrations of individual metal ions, do not dictate the overall budget of oxidizers, which is mostly modified through atmospheric deposition, agricultural and industrial runoff, and discharges from oil and gas platforms (Wurl et al., 2017). A study investigating the presence of nutrients and metals in waters of the North Sea attributed the highest metal content to the waters of the German Bight, source of the water used in the mesocosm study. Concentrations of redox-active metals, such as copper (Cu) and iron (Fe), were measured in values as high as 749 ng L<sup>-1</sup> and 150 ng L<sup>-1</sup> in this region (Siems et al., 2024). These metals have pronounced photochemical activity, and synergistic effects are known to play significant roles in their redox chemistry (Lueder et al., 2020; Deguillaume et al., 2005). To evaluate if these processes might have an influence in our observed results for the mesocosm study, the concentrations of Cu and Fe in SML and ULW samples were quantified. TXRF measurements demonstrated the presence of Cu and Fe in the pre-bloom phase (May 20<sup>th</sup>) and during the bloom (June 2<sup>nd</sup>). Cu concentrations in the SML and in the ULW were 0.3 and 0.2 μmol L<sup>-1</sup> on May 20<sup>th</sup>, and 0.5 and 0.3 μmol L<sup>-1</sup> on June 2<sup>nd</sup>. Fe concentrations in the SML and in the ULW were 1.2 and 1.0 μmol L<sup>-1</sup> on May 20<sup>th</sup>, 9.2 and 1.8 μmol L<sup>-1</sup> on June 2<sup>nd</sup>. Compared to those reported by Siems et al., we found slightly lower concentrations of Cu and much higher concentrations of Fe. As expected, the distribution of redox-active trace elements in the SML and ULW samples was relatively uniform. Previous studies have demonstrated that metal concentrations only decrease at higher water depths (Siems et al., 2024). These trace metal concentrations might contribute to the high observed redox activity of the samples in the in situ EPR experiments. However, further targeted studies are needed to quantify the relative role of metal ions and other redox-active components in seawater photooxidation:

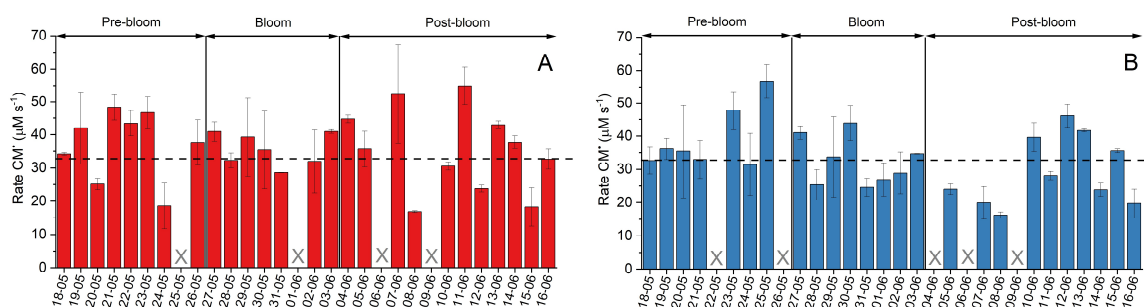


Figure 7: The overall CM radical formation in different samples after photon-flux correction for SML (A) and ULW (B) samples. The dashed line represents the mean CM radical formation rate considering all samples.

As shown in the Supplementary Information, Sect. S3, control experiments were conducted to verify the activity of Fe and Cu chloride salts, and a great contribution of Cu(I) and Cu(II) in the formation of CM radicals was observed, with formation rates reaching  $16 \mu\text{M s}^{-1}$  in the photolysis of a 500 nM CuCl solution. Fe(II) solutions showed no photoactivity, while Fe(III) showed a small contribution to CM radical formation, with maximum formation rates of  $0.2 \mu\text{M s}^{-1}$ . Although Cu ions were detected in the TXRF analysis, their presence alone does not account for the total observed photooxidation capacity of the samples. Considering the high reaction rates between CMH and  $\text{O}_2^-$ , and the absence of signals in the presence of DMPO, the formation of  $\text{O}_2^-$  is a strong candidate for the remaining CM radical formation rates. Measured formation rates calculated from the steady state concentrations of  $\text{O}_2^-$  radical considering CDOM photochemistry in natural ocean waters can reach  $480 \text{ nM h}^{-1}$  (Hansard et al., 2010), while OH radical formation rates reach  $110 \text{ nM h}^{-1}$  (Mopper and Zhou, 1990). In the EPR experiments, direct electron transfer from excited photosensitizers can also influence the results and contribute to the rate of CM formation.

Although the control experiments with Fe and Cu chloride salts indicate that Cu has a stronger effect on CMH oxidation than Fe, metal complexation significantly modulates the redox properties and the solubility of both Fe(III) and Cu(II) in seawater. In general, photoreduction is enhanced in the presence of ligands that form photoactive inner-sphere complexes and enable ligand-to-metal charge transfer (LMCT). While ligands, such as oxalate, are known to significantly increase the quantum yields for the metal reduction, this effect is much weaker for ligands with a lower stability constant (Sun et al., 1998). The solubility of Fe and Cu ions in ocean water is generally reduced in the absence of organic ligands due to the formation of hydroxy-oxo insoluble species promoted at typical seawater pH levels. Therefore, the presence of OM enhances the photochemistry of Fe and Cu in seawater by increasing the solubility of ions (Millero, 1998; Calza et al., 2014). However, OM itself comprises fulvic and humic acids, which have photosensitizing properties. Direct photosensitization processes can be suppressed when these photosensitizers are bound to Fe, since LMCT mechanisms will be favoured (Calza et al., 2014). Consequently, the overall effect of Cu and Fe complexation is very complex. Attributing the observed photooxidation to a decrease or increase in redox activity is not straightforward, and would require dedicated metal speciation and ligand characterization.

### 3.4 Implications for the ocean and the atmosphere

Carbonyl compounds can be transferred from the sea surface to the atmosphere due to their volatile nature, making air-sea exchanges of high relevance in their marine biogeochemical cycling. In general, the transfer of a compound from the liquid phase to the gas phase can be described using the two-layer model, which has been widely applied in the literature to estimate air-sea fluxes (Liss and Slater, 1974). In this model, the equilibrium concentrations of a compound in the gas ( $c_{sg}$ ) and in the liquid ( $c_{sl}$ ) at the interface are related through its apparent partition coefficient ( $H$ , in  $\text{M atm}^{-1}$ ), as expressed in Eq. (1):

$$H = \frac{c_{sl}}{c_{sg}}, \quad (1)$$

From the photochemical formation rates measured in the SML and the apparent partition coefficients (Table 2) compiled by Sander (Sander, 2023), the rates of transfer of photochemically produced carbonyl compounds from the SML ( $c_{sl}$ ) to the gas

interface ( $c_{sg}$ ) were estimated. Constant SML thickness of 100  $\mu\text{m}$  and temperature of 298 K were assumed for the calculations. Isovaleraldehyde and trans, trans-2,4-hexadienal were not considered due to the lack of published partition coefficient data.

630 The rates of transfer were calculated excluding the samples in which photochemical degradation rather than formation was observed; thus, we report no values for benzaldehyde and hexanal in the bloom phase. The non-bloom values in the table include both the pre-bloom and post-bloom phases of the mesocosm. A detailed explanation of the steps for the estimation of the rates of transfer to the gas interface are provided in the Supplementary Information, Sect. S5.

~~The estimated rates of transfer of carbonyl compounds from the SML to the atmosphere were generally higher during the bloom phase for the majority of the compounds, namely acrolein, biacetyl, butanal, crotonaldehyde, glyoxal, heptanal, methacrolein, methylglyoxal, MVK, propanal and trans 2 hexanal. This trend suggests that biological processes in the SML may also enhance the emission of VOCs to the atmosphere. However, for soluble compounds like glyoxal and methylglyoxal, their transfer into the gas phase is relatively low compared to other compounds with lower apparent partition coefficients. Although these compounds are photochemically produced in the SML, the net exchange direction is presumed to be predominantly from the atmosphere to the sea under typical atmospheric conditions (Zhou and Mopper, 1997). In contrast, the carbonyl compounds with three or more carbon atoms and low apparent partition coefficients (lower than  $10 \text{ M atm}^{-1}$ ) are the ones with the lowest solubilities and highest rates of transfer to the gas boundary layer, suggesting that their net flux is likely from the sea to the atmosphere (Zhou and Mopper, 1990b, 1997). Among these, propanal, butanal and octanal showed particularly high transfer rates to overlying atmosphere. Even though the photochemical activity of these compounds did not seem to be influenced by the phytoplankton bloom (see Sect. 3.2), their elevated rates of transfer to the gas phase suggest that the possibility of potential losses to the gas phase during the irradiation experiments should be considered. These compounds have been detected in both the sea surface and the overlying atmosphere (Schlundt et al., 2017), and models propose the Pacific Ocean as a major source of propanal to the atmosphere (Singh et al., 2003).~~

635  
640  
645  
650  
655  
660

**Table 2: Estimated rates of transfer of photochemically-produced carbonyl compounds from the SML to the gas interface ( $c_{st}$ ) according to equilibrium partitioning.**

Compound	Apparent partition coefficient (M atm <sup>-1</sup> )	Rate of transfer – Non-bloom (molecules cm <sup>-2</sup> h <sup>-1</sup> )	Rate of transfer - Bloom (molecules cm <sup>-2</sup> h <sup>-1</sup> )
Acetophenone	110 <sup>1</sup>	2 – 38 (× 10 <sup>2</sup> )	2 – 11 (× 10 <sup>2</sup> )
Acrolein	7.4 <sup>2</sup>	11 – 5544 (× 10 <sup>3</sup> )	2 – 19 (× 10 <sup>6</sup> )
Benzaldehyde	33.5 <sup>3</sup>	9 – 13 (× 10 <sup>4</sup> )	Not available
Biacetyl*	65.5 <sup>1,2</sup>	16 – 119 (× 10 <sup>3</sup> )	12 – 200 (× 10 <sup>3</sup> )
Butanal	6.3 <sup>3</sup>	3 – 9 (× 10 <sup>5</sup> )	5 – 56 (× 10 <sup>5</sup> )
Crotonaldehyde	52 <sup>4</sup>	10 – 24 (× 10 <sup>4</sup> )	2 – 71 (× 10 <sup>4</sup> )
Glyoxal	360000 <sup>3</sup>	11 – 57	4 – 134
Heptanal	2.0 <sup>3</sup>	4 – 10 (× 10 <sup>5</sup> )	5 – 105 (× 10 <sup>5</sup> )
Hexanal	3.2 <sup>3</sup>	6 – 41 (× 10 <sup>5</sup> )	Not available
Methacrolein	6.5 <sup>5</sup>	8 – 151 (× 10 <sup>4</sup> )	2 – 258 (× 10 <sup>5</sup> )
Methylglyoxal	32000 <sup>3</sup>	24 – 289	40 – 428
Methyl vinyl ketone	41 <sup>5</sup>	7 – 68 (× 10 <sup>4</sup> )	8 – 711 (× 10 <sup>4</sup> )
Octanal	1.1 <sup>3</sup>	2 – 20 (× 10 <sup>5</sup> )	3 – 158 (× 10 <sup>4</sup> )
Propanal	10 <sup>3</sup>	9 – 15 (× 10 <sup>5</sup> )	11 – 382 (× 10 <sup>5</sup> )
Trans-2-hexenal	20 <sup>4</sup>	6 – 30 (× 10 <sup>3</sup> )	1 – 2 (× 10 <sup>4</sup> )

\*Average value; <sup>1</sup>(Betterson, 1991); <sup>2</sup>(Snider and Dawson, 1985); <sup>3</sup>(Zhou and Mopper, 1990b), measured in seawater; <sup>4</sup>(Buttery et al., 1971); <sup>5</sup>(Iraci et al., 1999)

665

670

675

The estimated rates of transfer of photochemically-produced carbonyl compounds from the SML to the atmosphere according to equilibrium partitioning were generally higher during the bloom phase for the majority of the compounds, namely acrolein, biacetyl, butanal, crotonaldehyde, glyoxal, heptanal, methacrolein, methylglyoxal, MVK, propanal and trans-2-hexenal. This trend suggests that biological processes in the SML may also enhance the emission of VOCs to the atmosphere. However, for soluble compounds like glyoxal and methylglyoxal, their transfer into the gas phase is relatively low compared to other compounds with lower apparent partition coefficients. Although these compounds are photochemically produced in the SML, the net exchange direction is presumed to be predominantly from the atmosphere to the sea under typical atmospheric conditions (Zhou and Mopper, 1997). In contrast, the carbonyl compounds with three or more carbon atoms and low apparent partition coefficients (lower than 10 M atm<sup>-1</sup>) are the ones with the lowest solubilities and highest rates of transfer to the gas boundary layer, suggesting that their net flux is likely from the sea to the atmosphere (Zhou and Mopper, 1990b, 1997). Among these, propanal, butanal and octanal showed particularly high transfer rates to overlying atmosphere. Even though the photochemical activity of these compounds did not seem to be influenced by the phytoplankton bloom (see Sect. 3.2), their

680 elevated rates of transfer to the gas phase suggest that the possibility of potential losses to the gas phase during the irradiation experiments should be considered. These compounds have been detected in both the sea surface and the overlying atmosphere (Schlundt et al., 2017), and models propose the Pacific Ocean as a major source of propanal to the atmosphere (Singh et al., 2003).

685 Our results serve as a preliminary basis for refining air-sea exchange models, highlighting a potentially more significant role of the SML in the photochemical production of carbonyl compounds and its implications in the formation of SOAs. Considering the high transfer rates observed for several of the compounds in this study and their increase during the phytoplankton bloom, incorporating them into marine VOC inventories may help to reduce discrepancies between model predictions and real-world observations, especially in coastal areas where blooms are frequent. These results aim to serve as a preliminary basis for motivating new experimental efforts and refining air-sea exchange models, particularly by highlighting the role of the SML in the photochemical production of carbonyl compounds and its implications in the formation of SOAs.

690 We note that these estimations neglect the potential contribution of in situ loss processes within the SML, such as photolysis and microbial consumption, which may substantially decrease the fraction of photochemically-produced carbonyl compounds available for volatilization under ambient conditions. For this reason, the transfer rates presented in the present study shall be interpreted as upper-limit approximations.

695 While these transfer estimates based on equilibrium partitioning provide useful upper limits, an air-sea transfer estimate based on concentration gradients was explored for glyoxal as a case study, integrating measured SML concentrations under bloom and non-bloom conditions with representative atmospheric values (Supplementary Information, Sect. S5.2). The resulting transfer fluxes range between  $(1.7 - 20.8) \times 10^{-4} \text{ nmol cm}^{-2} \text{ s}^{-1}$  in non-bloom conditions, and  $(4.1 - 29.4) \times 10^{-4} \text{ nmol cm}^{-2} \text{ s}^{-1}$ . In contrast to the rates of transfer of photochemically-produced carbonyl compounds calculated using equilibrium partitioning (Sect. S5.1), the transfer fluxes estimated using the concentration gradient approach consider total glyoxal concentrations measured in the non-irradiated SML and in the atmosphere in the marine environment. This means that the gradient-based transfer fluxes reflex overall values that integrate all possible processes, while the results obtained in Sect. S5.1 are limited to the photochemically-produced compounds.

700 Overall, the increased transfer rates observed for several carbonyl compounds during the phytoplankton bloom highlight the need to incorporate the complex interplay of biotic and abiotic factors into marine VOC inventories, which may help to reduce discrepancies between model predictions and real-world observations, especially in coastal areas where blooms are frequent.

705 HoweverAdditionally, it is important to note that high production in the SML does not necessarily imply higher atmospheric concentrations. Because fluxes in the air-sea interface can be bidirectional, both emission and deposition processes should be taken into account when assessing the atmospheric significance of the SML photochemistry. Future experimental efforts should aim to quantify the photochemical production and volatilization of these carbonyl compounds simultaneously in both the gas and liquid phase to improve the accuracy of our estimations and evaluate more precisely the atmospheric impact of these processes.

710

#### 4 Summary and conclusions

The SML is a unique and dynamic environment characterized by its high concentrations of DOM and its direct exposure to strong solar radiation, making it a potential hotspot for photochemical reactions. In this study, we have assessed the photochemistry in SML and ULW samples collected in a mesocosm experiment where a phytoplankton bloom was induced by the controlled addition of inorganic nutrients. We explored two complementary aspects: (1) photochemical production of 17 atmospherically-relevant carbonyl compounds, and (2) overall photooxidation capacity of the system.

All the target carbonyl compounds were consistently enriched in the SML compared to ULW, supporting the role of the SML as a distinct habitat for abiotic processes. The concentrations in the SML of acetophenone, acrolein, biacetyl, butanal, crotonaldehyde, glyoxal, heptanal, hexanal, methacrolein, methylglyoxal, methyl vinyl ketone, octanal, propanal and trans-2-hexenal were higher during the phytoplankton bloom, which is likely the phase of the higher biological productivity and enrichment in reactive organic materials. The photochemical activity in the SML of acrolein, biacetyl, butanal, crotonaldehyde, glyoxal, heptanal, hexanal, methacrolein, methylglyoxal, methyl vinyl ketone, propanal and trans-2-hexenal (primarily isoprene- and lipid- derived products) was particularly higher under bloom conditions, suggesting a link between photochemical reactivity and bloom-induced DOM composition changes. The calculation of AQYs suggest that the SML is a more photochemically efficient environment compared to ULW, particularly in the bloom phase of the study. No systematic relationship was found between AQYs and DOC concentrations, which indicates that OM abundance alone does not control the efficiency of the investigated processes. The photochemical production rates of glyoxal and methylglyoxal calculated in this study are similar to those previously published under comparable conditions.

To complement these findings, we have evaluated the photooxidation capacity of SML and ULW samples in the along the mesocosm experiment via EPR spectroscopy, using a CMH probe to monitor the photochemical production of ROS and redox compounds. The estimated overall photooxidation rates remained similar in the three phases of the bloom, and they were comparable between the SML and ULW samples. After accounting for the differences on DOC levels measured along the mesocosm study, these results indicate that photooxidation capacity cannot be solely explained by variations of OM abundance. These results Instead, they suggest ~~that the photooxidation capacity in the samples was primarily driven by the preseneea~~ dominance of redox-active species, such as metal ions, rather than by biological processes.

Overall, our findings reveal that phytoplankton blooms enhance photochemical production of carbonyl compounds in the SML, but appear to have limited direct impact in the photooxidation capacity of these systems. These results suggest that photochemistry in the SML is governed by the complex interaction between biological activity and chemical composition, including DOM and redox-active species such as trace metals. Our work provides a novel perspective on how photochemical processes respond to biological events in the sea-surface, and points to them as potential sources of VOCs to the marine atmosphere.

While our observations are based on a single mesocosm study, further field verification of our findings are necessary to explore how broader environmental factors, such as nutrient availability, phytoplankton composition, temperature, wind stress, solar radiation and trace metals, can also influence these processes regionally and globally.

*Author contributions:* The study was conceptualized by OJV, DF, TS, MvP and HH. OJV and DF wrote the manuscript with contributions from TS, MvP, KWF and HH. OJV participated in the mesocosm study where the seawater samples were collected. OJV optimized the presented analytical method for carbonyl compound quantification with support from MvP, performed the experiments and treated the data with support from MvP and TS. DF developed the analytical method for the measurement of the photooxidation capacity, performed the experiments and treated the data. KWF developed the method for the trace metals analysis, performed the experiments and treated the data. All co-authors proofread and commented on the manuscript.

*Conflict of interest:* The authors declare that they have no conflict of interest.

*Acknowledgements:* We gratefully acknowledge the funding by the Deutsche Forschungsgemeinschaft (DFG, German Research Foundation) for the BASS project in subproject 1.4. (Grant N° 451574234 and HE3086/54-1), and the ANR/DFG project REACTE (HE3086/55-1). We thank Sylvia Haferkorn, Frederik Nowak and Elena Poschart for supporting the optimization of the GC-MS method and for fruitful discussions. We also thank Bochao Yang for his support in the measurement of samples using EPR spectroscopy. We thank the ICBM for the possibility to use their infrastructure during the mesocosm study.

*Financial support:* This research was supported by the project “Biogeochemical processes and Air-sea exchange in the Sea-Surface microlayer (BASS)”, which was funded by the Deutsche Forschungsgemeinschaft (DFG, German Research Foundation) under Grant N° 451574234 and HE3086/54-1, and by the project REACTE, which was funded by the ANR/DFG under Grant N° HE3086/55-1.

## References

- Andrews, S. S., Caron, S., and Zafiriou, O. C.: Photochemical oxygen consumption in marine waters: A major sink for colored dissolved organic matter?, *Limnol. Oceanogr.*, 45, 267-277, doi: 10.4319/lo.2000.45.2.0267, 2000.
- Arangio, A. M., Tong, H. J., Socorro, J., Pöschl, U., and Shiraiwa, M.: Quantification of environmentally persistent free radicals and reactive oxygen species in atmospheric aerosol particles, *Atmos. Chem. Phys.*, 16, 13105-13119, doi: 10.5194/acp-16-13105-2016, 2016.

- 775 Atkinson, R.: Atmospheric chemistry of VOCs and NO<sub>x</sub>, *Atmos. Environ.*, 34, 2063-2101, doi: 10.1016/S1352-2310(99)00460-4, 2000.
- Balls, P. W.: Copper, lead and cadmium in coastal waters of the western North-Sea, *Mar. Chem.*, 15, 363-378, doi: 10.1016/0304-4203(85)90047-7, 1985.
- Berg, S. M., Whiting, Q. T., Herrli, J. A., Winkels, R., Wammer, K. H., and Remucal, C. K.: The Role of Dissolved Organic  
780 Matter Composition in Determining Photochemical Reactivity at the Molecular Level, *Environ. Sci. Technol.*, 53, 11725-11734, doi: 10.1021/acs.est.9b03007, 2019.
- Betterton, E. A.: The partitioning of ketones between the gas and aqueous phases, *Atmos. Environ. A, Gen. Top.*, 25, 1473-1477, doi: 10.1016/0960-1686(91)90006-S, 1991.
- Bianco, A., Sordello, F., Ehn, M., Vione, D., and Passananti, M.: Degradation of nanoplastics in the environment: Reactivity  
785 and impact on atmospheric and surface waters, *Sci. Total Environ.*, 742, doi: 10.1016/j.scitotenv.2020.140413, 2020.
- Bibi, R., Ribas-Ribas, M., Jaeger, L., Lehnert, C., Gassen, L., Cortés, E., Wollschläger, J., Thölen, C., Waska, H., Zöbelein, J., Brinkhoff, T., Athale, I., Röttgers, R., Novak, M., Engel, A., Barthelmeß, T., Karnatz, J., Reinthaler, T., Spriahailo, D., Friedrichs, G., Schäfer, F., and Wurl, O.: Biogeochemical Dynamics of the Sea-Surface Microlayer in a Multidisciplinary Mesocosm Study, *EGUsphere*, 2025, 1-53, doi: 10.5194/egusphere-2025-1773, 2025.
- 790 Boonprab, K., Matsui, K., Yoshida, M., Akakabe, Y., Chirapart, A., and Kajiwara, T.: C6-aldehyde formation by fatty acid hydroperoxide lyase in the brown alga *Laminaria angustata*, *Z. Naturforsch. C.*, 58, 207-214, doi: 10.1515/znc-2003-3-412, 2003.
- Briedé, J. J., De Kok, T. M. C. M., Hogervorst, J. G. F., Moonen, E. J. C., Den Camp, C. L. B. O., and Kleinjans, J. C. S.: Development and application of an electron spin resonance spectrometry method for the determination of oxygen free radical  
795 formation by particulate matter, *Environ. Sci. Technol.*, 39, 8420-8426, doi: 10.1021/es0485311, 2005.
- Buttery, R. G., Bomben, J. L., Guadagni, D. G., and Ling, L. C.: Volatilities of organic flavor compounds in foods, *J. Agr. Food Chem.*, 19, 1045-1048, doi: 10.1021/jf60178a004, 1971.
- Calza, P., Vione, D., and Minero, C.: The role of humic and fulvic acids in the phototransformation of phenolic compounds in seawater, *Sci. Total Environ.*, 493, 411-418, doi: 10.1016/j.scitotenv.2014.05.145, 2014.
- 800 Carpenter, L. J. and Nightingale, P. D.: Chemistry and Release of Gases from the Surface Ocean, *Chem. Rev.*, 115, 4015-4034, doi: 10.1021/cr5007123, 2015.
- Cho, K., Ueno, M., Liang, Y., Kim, D., and Oda, T.: Generation of Reactive Oxygen Species (ROS) by Harmful Algal Bloom (HAB)-Forming Phytoplankton and Their Potential Impact on Surrounding Living Organisms, *Antioxidants*, 11, doi: 10.3390/antiox11020206, 2022.
- 805 Chu, C. H., Lundeen, R. A., Remucal, C. K., Sander, M., and McNeill, K.: Enhanced Indirect Photochemical Transformation of Histidine and Histamine through Association with Chromophoric Dissolved Organic Matter, *Environ. Sci. Technol.*, 49, 5511-5519, doi: 10.1021/acs.est.5b00466, 2015.

- Ciuraru, R., Fine, L., van Pinxteren, M., D'Anna, B., Herrmann, H., and George, C.: Unravelling New Processes at Interfaces: Photochemical Isoprene Production at the Sea Surface, *Environ. Sci. Technol.*, 49, 13199-13205, doi: 10.1021/acs.est.5b02388, 2015.
- 810 Coble, P. G.: Marine Optical Biogeochemistry: The Chemistry of Ocean Color, *Chem. Rev.*, 107, 402-418, doi: 10.1021/cr050350+, 2007.
- Conte, L., Szopa, S., Aumont, O., Gros, V., and Bopp, L.: Sources and Sinks of Isoprene in the Global Open Ocean: Simulated Patterns and Emissions to the Atmosphere, *J. Geophys. Res. Oceans*, 125, doi: 10.1029/2019JC015946, 2020.
- 815 Dai, Y., Yang, S. B., Zhao, D., Hu, C. M., Xu, W., Anderson, D. M., Li, Y., Song, X. P., Boyce, D. G., Gibson, L., Zheng, C. M., and Feng, L.: Coastal phytoplankton blooms expand and intensify in the 21st century, *Nature*, 615, 280-284, doi: 10.1038/s41586-023-05760-y, 2023.
- Dalrymple, R. M., Carfagno, A. K., and Sharpless, C. M.: Correlations between Dissolved Organic Matter Optical Properties and Quantum Yields of Singlet Oxygen and Hydrogen Peroxide, *Environ. Sci. Technol.*, 44, 5824-5829, doi: 820 10.1021/es101005u, 2010.
- Davidson, M. R., Mitchell, S. A., and Bradley, R. H.: Surface studies of low molecular weight photolysis products from UV-ozone oxidised polystyrene, *Surf. Sci.*, 581, 169-177, doi: 10.1016/j.susc.2005.02.049, 2005.
- de Bruyn, W. J., Clark, C. D., Pagel, L., and Takehara, C.: Photochemical production of formaldehyde, acetaldehyde and acetone from chromophoric dissolved organic matter in coastal waters, *J. Photoch. Photobio. A*, 226, 16-22, doi: 825 10.1016/j.jphotochem.2011.10.002, 2011.
- de Bruyn, W. J., Clark, C. D., Senstad, M., Barashy, O., and Hok, S.: The biological degradation of acetaldehyde in coastal seawater, *Mar. Chem.*, 192, 13-21, doi: 10.1016/j.marchem.2017.02.008, 2017.
- Deguillaume, L., Leriche, M., Desboeufs, K., Mailhot, G., George, C., and Chaumerliac, N.: Transition metals in atmospheric liquid phases: Sources, reactivity, and sensitive parameters, *Chem. Rev.*, 105, 3388-3431, doi: 10.1021/cr040649c, 2005.
- 830 Dixon, J. L., Beale, R., Sargeant, S. L., Tarran, G. A., and Nightingale, P. D.: Microbial acetone oxidation in coastal seawater, *Front. Microbiol.*, 5, doi: 10.3389/fmicb.2014.00243, 2014.
- Duinker, J. C. and Nolting, R. F.: Dissolved copper, zinc and cadmium in the Southern Bight of the North Sea, *Mar. Pollut. Bull.*, 13, 93-96, doi: 10.1016/0025-326x(82)90199-0, 1982.
- Ehrhardt, M. and Petrick, G.: On the sensitized photo-oxidation of alkylbenzenes in seawater, *Mar. Chem.*, 15, 47-58, doi: 835 10.1016/0304-4203(84)90037-9, 1984.
- Ehrhardt, M., Bouchertall, F., and Hopf, H. P.: Aromatic ketones concentrated from Baltic Sea water, *Mar. Chem.*, 11, 449-461, doi: 10.1016/0304-4203(82)90010-X, 1982.
- Engel, A., Bange, H. W., Cunliffe, M., Burrows, S. M., Friedrichs, G., Galgani, L., Herrmann, H., Hertkorn, N., Johnson, M., Liss, P. S., Quinn, P. K., Schartau, M., Soloviev, A., Stolle, C., Upstill-Goddard, R. C., van Pinxteren, M., and Zäncker, B.: 840 The Ocean's Vital Skin: Toward an Integrated Understanding of the Sea Surface Microlayer, *Front Mar Sci*, 4, 10.3389/fmars.2017.00165, 2017.

- Epstein, S. A., Tapavicza, E., Furche, F., and Nizkorodov, S. A.: Direct photolysis of carbonyl compounds dissolved in cloud and fog droplets, *Atmos. Chem. Phys.*, 13, 9461-9477, doi: 10.5194/acp-13-9461-2013, 2013.
- 845 Fabbri, D., Carena, L., Bertone, D., Brigante, M., Passananti, M., and Vione, D.: Assessing the photodegradation potential of compounds derived from the photoinduced weathering of polystyrene in water, *Sci. Total Environ.*, 876, doi: 10.1016/j.scitotenv.2023.162729, 2023.
- Ferrario, J. B., Lawler, G. C., Deleon, I. R., and Laseter, J. L.: Volatile Organic Pollutants in Biota and Sediments of Lake Pontchartrain, *Bull. Environ. Contam. Toxicol.*, 34, 246-255, doi: 10.1007/BF01609730, 1985.
- 850 Fomba, K. W., Müller, K., van Pinxteren, D., and Herrmann, H.: Aerosol size-resolved trace metal composition in remote northern tropical Atlantic marine environment: case study Cape Verde islands, *Atmos. Chem. Phys.*, 13, 4801-4814, doi: 10.5194/acp-13-4801-2013, 2013.
- Fomba, K. W., Deabji, N., Barcha, S. E., Ouchen, I., Elbaramoussi, E., El Moursli, R. C., Harnafi, M., El Hajjaji, S., Mellouki, A., and Herrmann, H.: Application of TXRF in monitoring trace metals in particulate matter and cloud water, *Atmos. Meas. Tech.*, 13, 4773-4790, doi: 10.5194/amt-13-4773-2020, 2020.
- 855 Fu, T. M., Jacob, D. J., Wittrock, F., Burrows, J. P., Vrekoussis, M., and Henze, D. K.: Global budgets of atmospheric glyoxal and methylglyoxal, and implications for formation of secondary organic aerosols, *J. Geophys. Res. Atmos.*, 113, doi: 10.1029/2007jd009505, 2008.
- Fujii, M. and Otani, E.: Photochemical generation and decay kinetics of superoxide and hydrogen peroxide in the presence of standard humic and fulvic acids, *Water Res.*, 123, 642-654, doi: 10.1016/j.watres.2017.07.015, 2017.
- 860 González-Davila, M., Santana-Casiano, J. M., and Millero, F. J.: Oxidation of iron (II) nanomolar with H<sub>2</sub>O<sub>2</sub> in seawater, *Geochim. Cosmochim. Acta*, 68, A377-A377, doi: 10.1016/j.gca.2004.05.043, 2004.
- Gotham, J. P., Li, R., Tipple, T. E., Lancaster, J. r., Liu, T. M., and Li, Q.: Quantitation of spin probe-detectable oxidants in cells using electron paramagnetic resonance spectroscopy: To probe or to trap?, *Free Radic. Bio. Med.*, 154, 84-94, doi: 10.1016/j.freeradbiomed.2020.04.020, 2020.
- 865 Grandbois, M., Latch, D. E., and Mcneill, K.: Microheterogeneous Concentrations of Singlet Oxygen in Natural Organic Matter Isolate Solutions, *Environ. Sci. Technol.*, 42, 9184-9190, doi: 10.1021/es8017094, 2008.
- Hansard, S. P., Vermilyea, A. W., and Voelker, B. M.: Measurements of superoxide radical concentration and decay kinetics in the Gulf of Alaska, *Deep-Sea Res. I*, 57, 1111-1119, doi: 10.1016/j.dsr.2010.05.007, 2010.
- Hansel, C. M. and Diaz, J. M.: Production of Extracellular Reactive Oxygen Species by Marine Biota, *Annu. Rev. Mar. Sci.*, 870 13, 177-200, doi: 10.1146/annurev-marine-041320-102550, 2021.
- Hansell, D. A. and Carlson, C. A.: *Biogeochemistry of Marine Dissolved Organic Matter*, Academic Press, London 2002.
- Hardy, J. T.: The sea-surface microlayer: Biology, chemistry and anthropogenic enrichment, *Prog. Oceanogr.*, 11, 307-328, doi: 10.1016/0079-6611(82)90001-5, 1982.
- Harvey, G. W. and Burzell, L. A.: Simple Microlayer Method for Small Samples, *Limnol. Oceanogr.*, 17, 156-157, doi: 875 10.4319/lo.1972.17.1.0156, 1972.

- Hatchard, C. G. and Parker, C. A.: A New Sensitive Chemical Actinometer. II. Potassium Ferrioxalate as a Standard Chemical Actinometer, *Proc. R. Soc. Lon. A Math. Phys. Sci.*, 235, 518-536, doi: 10.1098/rspa.1956.0102, 1956.
- Huang, D., Zhang, X., Chen, Z. M., Zhao, Y., and Shen, X. L.: The kinetics and mechanism of an aqueous phase isoprene reaction with hydroxyl radical, *Atmos. Chem. Phys.*, 11, 7399-7415, doi: 10.5194/acp-11-7399-2011, 2011.
- 880 Iraci, L. T., Baker, B. M., Tyndall, G. S., and Orlando, J. J.: Measurements of the Henry's law coefficients of 2-Methyl-3-buten-2-ol, Methacrolein, and Methylvinyl ketone, *J. Atmos. Chem.*, 33, 321-330, doi: 10.1023/A:1006169029230, 1999.
- Jaoui, M., Nestorowicz, K., Rudzinski, K. J., Lewandowski, M., Kleindienst, T. E., Torres, J., Bulska, E., Danikiewicz, W., and Szmigielski, R.: Atmospheric oxidation of 1,3-butadiene: influence of seed aerosol acidity and relative humidity on SOA composition and the production of air toxic compounds, *Atmos. Chem. Phys.*, 25, 1401-1432, doi: 10.5194/acp-25-1401-2025, 885 2025.
- Jiménez, E., Lanza, B., Martínez, E., and Albaladejo, J.: Daytime tropospheric loss of hexanal and trans-2-hexenal: OH kinetics and UV photolysis, *Atmos. Chem. Phys.*, 7, 1565-1574, doi: 10.5194/acp-7-1565-2007, 2007.
- Jomova, K. and Valko, M.: Advances in metal-induced oxidative stress and human disease, *Toxicology*, 283, 65-87, doi: 10.1016/j.tox.2011.03.001, 2011.
- 890 Kato, S., Shimizu, N., Otoki, Y., Ito, J., Sakaino, M., Sano, T., Takeuchi, S., Imagi, J., and Nakagawa, K.: Determination of acrolein generation pathways from linoleic acid and linolenic acid: increment by photo irradiation, *Npj Sci. Food*, 6, doi: 10.1038/s41538-022-00138-2, 2022.
- Kieber, R. J., Zhou, X. L., and Mopper, K.: Formation of carbonyl compounds from UV-Induced photodegradation of humic substances in natural waters: Fate of riverine carbon in the sea, *Limnol. Oceanogr.*, 35, 1503-1515, doi: 895 10.4319/lo.1990.35.7.1503, 1990.
- Kilgour, D. B., Novak, G. A., Claflin, M. S., Lerner, B. M., and Bertram, T. H.: Production of oxygenated volatile organic compounds from the ozonolysis of coastal seawater, *Atmos. Chem. Phys.*, 24, 3729-3742, doi: 10.5194/acp-24-3729-2024, 2024.
- Kuhn, H. J., Braslavsky, S. E., and Schmidt, R.: Chemical actinometry, *Pure Appl. Chem.*, 76, 2105-2146, doi: 900 10.1351/pac200476122105, 2004.
- Lampert, W.: Release of dissolved organic carbon by grazing zooplankton, *Limnol. Oceanogr.*, 23, 831-834, doi: 10.4319/lo.1978.23.4.0831, 1978.
- Lancelot, C.: Gross excretion rates of natural marine phytoplankton and heterotrophic uptake of excreted products in the southern North Sea, as determined by short-term kinetics, *Mar. Ecol. Prog. Ser.*, 1, 179-186, doi: 10.3354/meps001179, 1979.
- 905 Liss, P. S. and Slater, P. G.: Flux of Gases Across Air-Sea Interface, *Nature*, 247, 181-184, doi: 10.1038/247181a0, 1974.
- Liss, P. S., Watson, A. J., Bock, E. J., Jahne, B., Asher, W. E., Frew, N. M., Hasse, L., Korenowski, G. M., Merlivat, L., Phillips, L. F., Schluessel, P., and Woolf, D. K.: *The Sea Surface and Global Change*, Cambridge University Press, Cambridge 1997.

- Lueder, U., Jorgensen, B. B., Kappler, A., and Schmidt, C.: Photochemistry of iron in aquatic environments, *Environ. Sci.: Process. Impacts*, 22, 12-24, doi: 10.1039/c9em00415g, 2020.
- 910 Mart, L. and Nurnberg, H. W.: Cd, Pb, Cu, Ni and Co distribution in the German Bight, *Mar. Chem.*, 18, 197-213, doi: 10.1016/0304-4203(86)90008-3, 1986.
- McNeill, K. and Canonica, S.: Triplet state dissolved organic matter in aquatic photochemistry: reaction mechanisms, substrate scope, and photophysical properties, *Environ. Sci. Process. Impacts*, 18, 1381-1399, doi: 10.1039/c6em00408c, 2016.
- 915 Millero, F. J.: Solubility of Fe(III) in seawater, *Earth Planet. Sc. Lett.*, 154, 323-329, doi: 10.1023/A:100616902923010.1016/S0012-821x(97)00179-9, 1998.
- Millero, F. J., Sharma, V. K., and Karn, B.: The rate of reduction of copper(II) with hydrogen peroxide in seawater, *Mar. Chem.*, 36, 71-83, doi: 10.1016/S0304-4203(09)90055-X, 1991.
- Millero, F. J., Sotolongo, S., and Izaguirre, M.: The oxidation kinetics of Fe(II) in seawater, *Geochim. Cosmochim. Acta*, 51, 793-801, doi: 10.1016/0016-7037(87)90093-7, 1987.
- 920 Millet, D. B., Guenther, A., Siegel, D. A., Nelson, N. B., Singh, H. B., de Gouw, J. A., Warneke, C., Williams, J., Eerdekens, G., Sinha, V., Karl, T., Flocke, F., Apel, E., Riemer, D. D., Palmer, P. I., and Barkley, M.: Global atmospheric budget of acetaldehyde: 3-D model analysis and constraints from in-situ and satellite observations, *Atmos. Chem. Phys.*, 10, 3405-3425, doi: 10.5194/acp-10-3405-2010, 2010.
- 925 Milne, P. J., Riemer, D. D., Zika, R. G., and Brand, L. E.: Measurement of vertical distribution of isoprene in surface seawater, Its chemical fate, and its emission from several phytoplankton monocultures, *Mar. Chem.*, 48, 237-244, doi: 10.1016/0304-4203(94)00059-M, 1995.
- Moan, J., Hovik, B., and Wold, E.: Two New Methods of Actinometry for EPR-Measurements, *Photochem. Photobiol.*, 30, 623-624, doi: 10.1111/j.1751-1097.1979.tb07189.x, 1979.
- 930 Moffett, J. W. and Zika, R. G.: Oxidation kinetics of Cu(I) in seawater: implications for its existence in the marine environment, *Mar. Chem.*, 13, 239-251, doi: 10.1016/0304-4203(83)90017-8, 1983.
- Moffett, J. W. and Zika, R. G.: Reaction kinetics of hydrogen peroxide with copper and iron in seawater, *Environ. Sci. Technol.*, 21, 804-810, doi: 10.1021/es00162a012, 1987.
- Moise, T. and Rudich, Y.: Reactive Uptake of Ozone by Aerosol-Associated Unsaturated Fatty Acids: Kinetics, Mechanism, and Products, *J. Phys. Chem. A*, 106, 6469-6476, doi: 10.1021/jp025597e, 2002.
- 935 Momzikoff, A., Santus, R., and Giraud, M.: A study of the photosensitizing properties of seawater, *Mar. Chem.*, 12, 1-14, doi: 10.1016/0304-4203(83)90024-5, 1983.
- Moore, R. M., Oram, D. E., and Penkett, S. A.: Production of isoprene by marine phytoplankton cultures, *Geophys. Res. Lett.*, 21, 2507-2510, doi: 10.1029/94GL02363, 1994.
- 940 Mopper, K. and Stahovec, W. L.: Sources and sinks of low molecular weight organic carbonyl compounds in seawater, *Mar. Chem.*, 19, 305-321, doi: 10.1016/0304-4203(86)90052-6, 1986.

- Mopper, K. and Zhou, X. L.: Hydroxyl Radical Photoproduction in the Sea and Its Potential Impact on Marine Processes, *Science*, 250, 661-664, doi: 10.1126/science.250.4981.661, 1990.
- Mopper, K., Zhou, X. L., Kieber, R. J., Kieber, D. J., Sikorski, R. J., and Jones, R. D.: Photochemical degradation of dissolved  
945 organic carbon and its impact on the oceanic carbon cycle, *Nature*, 353, 60-62, doi: 10.1038/353060a0, 1991.
- Nishimura, T., Hara, K., Honda, N., Okazaki, S., Hazama, H., and Awazu, K.: Determination and analysis of singlet oxygen quantum yields of talaporfin sodium, protoporphyrin IX, and lipidated protoporphyrin IX using near-infrared luminescence spectroscopy, *Lasers Med. Sci.*, 35, 1289-1297, doi: 10.1007/s10103-019-02907-0, 2020.
- Nolting, R. F.: Copper, zinc, cadmium, nickel, iron and manganese in the Southern Bight of the North Sea, *Mar. Pollut. Bull.*,  
950 17, 113-117, doi: 10.1016/0025-326X(86)90415-7, 1986.
- Onyango, A. N.: Small reactive carbonyl compounds as tissue lipid oxidation products; and the mechanisms of their formation thereby, *Chem. Phys. Lipids*, 165, 777-786, doi: 10.1016/j.chemphyslip.2012.09.004, 2012.
- Penezic, A., Wang, X. K., Perrier, S., George, C., and Frka, S.: Interfacial photochemistry of marine diatom lipids: Abiotic production of volatile organic compounds and new particle formation, *Chemosphere*, 313, doi:  
955 10.1016/j.chemosphere.2022.137510, 2023.
- Rabani, J., Mamane, H., Pousty, D., and Bolton, J. R.: Practical Chemical Actinometry - A Review, *Photochem. Photobiol.*, 97, 873-902, doi: 10.1111/php.13429, 2021.
- Rocco, M., Dunne, E., Peltola, M., Barr, N., Williams, J., Colomb, A., Safi, K., Saint-Macary, A., Marriner, A., Deppeler, S., Harnwell, J., Law, C., and Sellegri, K.: Oceanic phytoplankton are a potentially important source of benzenoids to the remote  
960 marine atmosphere, *Commun. Earth Environ.*, 2, doi: 10.1038/s43247-021-00253-0, 2021.
- Rochelle-Newall, E. J., Fisher, T. R., Fan, C., and Glibert, P. M.: Dynamics of chromophoric dissolved organic matter and dissolved organic carbon in experimental mesocosms, *Int. J. Remote Sens.*, 20, 627-641, doi: 10.1080/014311699213389, 1999.
- Rodigast, M., Mutzel, A., Iinuma, Y., Haferkorn, S., and Herrmann, H.: Characterisation and optimisation of a sample  
965 preparation method for the detection and quantification of atmospherically relevant carbonyl compounds in aqueous medium, *Atmos. Meas. Tech.*, 8, 2409-2416, doi: 10.5194/amt-8-2409-2015, 2015.
- Sander, R.: Compilation of Henry's law constants (version 5.0.0) for water as solvent, *Atmos. Chem. Phys.*, 23, 10901-12440, doi: 10.5194/acp-23-10901-2023, 2023.
- Scheres Firak, D., Schaefer, T., Yang, B., Jibaja Valderrama, O., van Pinxteren, M., and Herrmann, H.: Coupling Chemical  
970 Actinometry with EPR Spectroscopy: An Approach for Probing Photochemical Processes at the Air-Sea Interface, *ChemPhysChem.*, in press.
- Schlundt, C., Tegtmeier, S., Lennartz, S. T., Bracher, A., Cheah, W., Krüger, K., Quack, B., and Marandino, C. A.: Oxygenated volatile organic carbon in the western Pacific convective center: ocean cycling, air-sea gas exchange and atmospheric transport, *Atmos. Chem. Phys.*, 17, 10837-10854, doi: 10.5194/acp-17-10837-2017, 2017.

- 975 Schobert, B. and Elstner, E. F.: Production of Hexanal and Ethane by *Phaeodactylum-Triconutum* and Its Correlation to Fatty Acid Oxidation and Bleaching of Photosynthetic Pigments, *Plant Physiol.*, 66, 215-219, doi: 10.1104/pp.66.2.215, 1980.
- Scully, N. M., McQueen, D. J., Lean, D. R. S., and Cooper, W. J.: Hydrogen peroxide formation: The interaction of ultraviolet radiation and dissolved organic carbon in lake waters along a 43-75°N gradient, *Limnol. Oceanogr.*, 41, 540-548, doi: 10.4319/lo.1996.41.3.0540, 1996.
- 980 Sharma, V. K. and Millero, F. J.: Oxidation of copper(I) in seawater, *Environ. Sci. Technol.*, 22, 768-771, doi: 10.1021/es00172a004, 1988.
- Shaw, S. L., Chisholm, S. W., and Prinn, R. G.: Isoprene production by *Prochlorococcus*, a marine cyanobacterium, and other phytoplankton, *Mar. Chem.*, 80, 227-245, doi: 10.1016/S0304-4203(02)00101-9, 2003.
- Siems, A., Zimmermann, T., Sanders, T., and Pröfrock, D.: Dissolved trace elements and nutrients in the North Sea - A current baseline, *Environ. Monit. Assess.*, 196, doi: 10.1007/s10661-024-12675-2, 2024.
- 985 Simó, R., Cortés-Greus, P., Rodríguez-Ros, P., and Masdeu-Navarro, M.: Substantial loss of isoprene in the surface ocean due to chemical and biological consumption, *Commun. Earth Environ.*, 3, doi: 10.1038/s43247-022-00352-6, 2022.
- Singh, H. B., Tabazadeh, A., Evans, M. J., Field, B. D., Jacob, D. J., Sachse, G., Crawford, J. H., Shetter, R., and Brune, W. H.: Oxygenated volatile organic chemicals in the oceans: Inferences and implications based on atmospheric observations and air-sea exchange models, *Geophys. Res. Lett.*, 30, doi: 10.1029/2003gl017933, 2003.
- 990 Sinha, V., Williams, J., Meyerhöfer, M., Riebesell, U., Paulino, A. I., and Larsen, A.: Air-sea fluxes of methanol, acetone, acetaldehyde, isoprene and DMS from a Norwegian fjord following a phytoplankton bloom in a mesocosm experiment, *Atmos. Chem. Phys.*, 7, 739-755, doi: 10.5194/acp-7-739-2007, 2007.
- Snider, J. R. and Dawson, G. A.: Tropospheric light alcohols, carbonyls, and acetonitrile: Concentrations in southwestern United States and Henry's Law data, *J. Geophys. Res. Atmos.*, 90, 3797-3805, doi: 10.1029/JD090iD02p03797, 1985.
- 995 Sun, L. H., Wu, C. H., and Faust, B. C.: Photochemical redox reactions of inner-sphere copper(II)-dicarboxylate complexes: Effects of the dicarboxylate ligand structure on copper(I) quantum yields, *J. Phys. Chem. A*, 102, 8664-8672, doi: 10.1023/A:100616902923010.1021/jp982045g, 1998.
- Sun, L. N., Qian, J. G., Blough, N. V., and Mopper, K.: Insights into the Photoproduction Sites of Hydroxyl Radicals by Dissolved Organic Matter in Natural Waters, *Environ. Sci. Technol. Lett.*, 2, 352-356, doi: 10.1021/acs.estlett.5b00294, 2015.
- 1000 Tadic, J., Juranic, I., and Moortgat, G. K.: Photooxidation of n-Hexanal in Air, *Molecules*, 6, 287-299, doi: 10.3390/60400287, 2001.
- Thölen, C., Wollschläger, J., Novak, M. G., Röttgers, R., and Zielinski, O.: Colored and Fluorescent DOM in the Sea-Surface Microlayer: Response to a Phytoplankton Bloom and Photodegradation in a Mesocosm Study, *EGU sphere*, 2026, 1-39, doi: 10.5194/egusphere-2025-5350, 2026.
- 1005 Thomalla, S. J., Nicholson, S. A., Ryan-Keogh, T. J., and Smith, M. E.: Widespread changes in Southern Ocean phytoplankton blooms linked to climate drivers, *Nat. Clim. Change*, 13, 975-984, doi: 10.1038/s41558-023-01768-4, 2023.

- Thornberry, T. and Abbatt, J. P. D.: Heterogeneous reaction of ozone with liquid unsaturated fatty acids: detailed kinetics and gas-phase product studies, *Phys. Chem. Chem. Phys.*, 6, 84-93, doi: 10.1039/b310149e, 2004.
- 1010 Tilgner, A. and Herrmann, H.: Radical-driven carbonyl-to-acid conversion and acid degradation in tropospheric aqueous systems studied by CAPRAM, *Atmos. Environ.*, 44, 5415-5422, doi: 10.1016/j.atmosenv.2010.07.050, 2010.
- Tinel, L., Abbatt, J., Saltzman, E., Engel, A., Fernandez, R., Li, Q. Y., Mahajan, A. S., Nicewonger, M., Novak, G., Saiz-Lopez, A., Schneider, S., and Wang, S. S.: Impacts of ocean biogeochemistry on atmospheric chemistry, *Elem. Sci. Anth.*, 11, doi: 10.1525/elementa.2023.00032, 2023.
- 1015 Tuazon, E. C., Macleod, H., Atkinson, R., and Carter, W. P. L.: Alpha-Dicarbonyl Yields from the NO<sub>x</sub>-Air Photooxidations of a Series of Aromatic-Hydrocarbons in Air, *Environ. Sci. Technol.*, 20, 383-387, doi: 10.1021/es00146a010, 1986.
- Tuazon, E. C., Alvarado, A., Aschmann, S. M., Atkinson, R., and Arey, J.: Products of the Gas-Phase Reactions of 1,3-Butadiene with OH and NO<sub>3</sub> Radicals, *Environ. Sci. Technol.*, 33, 3586-3595, doi: 10.1021/es990193u, 1999.
- Uchida, K., Kanematsu, M., Morimitsu, Y., Osawa, T., Noguchi, N., and Niki, E.: Acrolein Is a Product of Lipid Peroxidation Reaction: Formation of Free Acrolein and Its Conjugate with Lysine Residues in Oxidized Low Density Lipoproteins, *J. Biol. Chem.*, 273, 16058-16066, doi: 10.1074/jbc.273.26.16058, 1998.
- 1020 van Pinxteren, M. and Herrmann, H.: Glyoxal and methylglyoxal in Atlantic seawater and marine aerosol particles: method development and first application during the Polarstern cruise ANT XXVII/4, *Atmos. Chem. Phys.*, 13, 11791-11802, doi: 10.5194/acp-13-11791-2013, 2013.
- 1025 Vaughan, P. P. and Blough, N. V.: Photochemical Formation of Hydroxyl Radical by Constituents of Natural Waters, *Environ. Sci. Technol.*, 32, 2947-2953, doi: 10.1021/es9710417, 1998.
- Volkamer, R., Platt, U., and Wirtz, K.: Primary and Secondary Glyoxal Formation from Aromatics: Experimental Evidence for the Bicycloalkyl-Radical Pathway from Benzene, Toluene, and *p*-Xylene, *J. Phys. Chem. A*, 105, 7865-7874, doi: 10.1021/jp010152w, 2001.
- 1030 Waggoner, D. C., Wozniak, A. S., Cory, R. M., and Hatcher, P. G.: The role of reactive oxygen species in the degradation of lignin derived dissolved organic matter, *Geochim. Cosmochim. Acta*, 208, 171-184, doi: 10.1016/j.gca.2017.03.036, 2017.
- Wagner, S., Schubotz, F., Kaiser, K., Hallmann, C., Waska, H., Rossel, P. E., Hansmann, R., Elvert, M., Middelburg, J. J., Engel, A., Blattmann, T. M., Catalá, T. S., Lennartz, S. T., Gomez-Saez, G. V., Pantoja-Gutiérrez, S., Bao, R., and Galy, V.: Soothsaying DOM: A Current Perspective on the Future of Oceanic Dissolved Organic Carbon, *Front. Mar. Sci.*, 7, doi: 10.3389/fmars.2020.00341, 2020.
- 1035 Walker, H., Stone, D., Ingham, T., Hackenberg, S., Cryer, D., Punjabi, S., Read, K., Lee, J., Whalley, L., Spracklen, D., Carpenter, L. J., Arnold, S. R., and Heard, D. E.: Observations and modelling of glyoxal in the tropical Atlantic marine boundary layer, *Atmos. Chem. Phys.*, 22, 5535-5557, doi: 10.5194/acp-22-5535-2022, 2022.
- Wang, S. Y., Hornbrook, R. S., Hills, A., Emmons, L. K., Tilmes, S., Lamarque, J. F., Jimenez, J. L., Campuzano-Jost, P., 1040 Nault, E. A., Crounse, J. D., Wennberg, P. O., Kim, M., Allen, H., Ryerson, T. B., Thompson, C. R., Peischl, J., Moore, F., Nance, D., Hall, B., Elkins, J., Tanner, D., Huey, L. G., Hall, S. R., Ullmann, K., Orlando, J. J., Tyndall, G. S., Flocke, F. M.,

- Ray, E., Hanisco, T. F., Wolfe, G. M., St Clair, J., Commane, R., Daube, B., Barletta, B., Blake, D. R., Weinzierl, B., Dollner, M., Conley, A., Vitt, F., Wofsy, S. C., Riemer, D. D., and Apel, E. C.: Atmospheric Acetaldehyde: Importance of Air-Sea Exchange and a Missing Source in the Remote Troposphere, *Geophys. Res. Lett.*, 46, 5601-5613, doi: 10.1029/2019gl082034, 1045 2019.
- Wang, Y. Q., Zeng, J. Q., Wu, B. J., Song, W., Hu, W. W., Liu, J. P., Yang, Y., Yu, Z. Q., Wang, X. M., and Gligorovski, S.: Production of Volatile Organic Compounds by Ozone Oxidation Chemistry at the South China Sea Surface Microlayer, *ACS Earth Space Chem.*, 7, 1306-1313, doi: 10.1021/acsearthspacechem.3c00102, 2023.
- Williams, R. T., Caspers-Brown, A., Michaud, J., Stevens, N., Meehan, M., Sultana, C. M., Lee, C. S. P., Malfatti, F., Zhou, Y. Y., Azam, F., Prather, K. A., Dorrestein, P., Burkart, M. D., and Pomeroy, R. S.: Possible Missing Sources of Atmospheric Glyoxal Part II: Oxidation of Toluene Derived from the Primary Production of Marine Microorganisms, *Metabolites*, 14, doi: 1050 3110.3390/metabo14110631, 2024.
- Wu, H. Y. and Lin, J. K.: Determination of Aldehydic Lipid Peroxidation Products with Dabsylhydrazine by High-Performance Liquid Chromatography, *Anal. Chem.*, 67, 1603-1612, doi: 10.1021/ac00105a020, 1995.
- 1055 Wurl, O., Ekau, W., Landing, W. M., and Zappa, C. J.: Sea-surface microlayer in a changing ocean - A perspective, *Elem. Sci. Anth.*, 5, doi: 10.1525/elementa.228/112437, 2017.
- Wurl, O., Stolle, C., Van Thuoc, C., Thu, P. T., and Mari, X.: Biofilm-like properties of the sea surface and predicted effects on air-sea CO<sub>2</sub> exchange, *Prog. Oceanogr.*, 144, 15-24, doi: 10.1016/j.pocean.2016.03.002, 2016.
- Wurl, O., Wurl, E., Miller, L., Johnson, K., and Vagle, S.: Formation and global distribution of sea-surface microlayers, 1060 *Biogeosciences*, 8, 121-135, doi: 10.5194/bg-8-121-2011, 2011.
- Yang, L., Zhang, J., Engel, A., and Yang, G. P.: Spatio-temporal distribution, photoreactivity and environmental control of dissolved organic matter in the sea-surface microlayer of the eastern marginal seas of China, *Biogeosciences*, 19, 5251-5268, doi: 10.5194/bg-19-5251-2022, 2022.
- Zafiriou, O. C.: Marine organic photochemistry previewed, *Mar. Chem.*, 5, 497-522, doi: 10.1016/0304-4203(77)90037-8, 1065 1977.
- Zhang, Y., Del Vecchio, R., and Blough, N. V.: Investigating the Mechanism of Hydrogen Peroxide Photoproduction by Humic Substances, *Environ. Sci. Technol.*, 46, 11836-11843, doi: 10.1021/es3029582, 2012.
- Zhou, S., Gonzalez, L., Leithead, A., Finewax, Z., Thalman, R., Vlasenko, A., Vagle, S., Miller, L. A., Li, S. M., Bureekul, S., Furutani, H., Uematsu, M., Volkamer, R., and Abbatt, J.: Formation of gas-phase carbonyls from heterogeneous oxidation 1070 of polyunsaturated fatty acids at the air-water interface and of the sea-surface microlayer, *Atmos. Chem. Phys.*, 14, 1371-1384, doi: 10.5194/acp-14-1371-2014, 2014.
- Zhou, X. L. and Mopper, K.: Determination of photochemically produced hydroxyl radicals in seawater and Freshwater, *Mar. Chem.*, 30, 71-88, doi: 10.1016/0304-4203(90)90062-H, 1990a.

- Zhou, X. L. and Mopper, K.: Apparent Partition-Coefficients of 15 Carbonyl Compounds between Air and Seawater and  
1075 between Air and Freshwater; Implications for Air Sea Exchange, *Environ. Sci. Technol.*, 24, 1864-1869, doi:  
10.1021/es00082a013, 1990b.
- Zhou, X. L. and Mopper, K.: Photochemical production of low-molecular-weight carbonyl compounds in seawater and surface  
microlayer and their air-sea exchange, *Mar. Chem.*, 56, 201-213, doi: 10.1016/S0304-4203(96)00076-X, 1997.
- Zhu, Y. T. and Kieber, D. J.: Wavelength- and Temperature-Dependent Apparent Quantum Yields for Photochemical  
1080 Production of Carbonyl Compounds in the North Pacific Ocean, *Environ. Sci. Technol.*, 52, 1929-1939, doi:  
10.1021/acs.est.7b05462, 2018.
- Zhu, Y. T. and Kieber, D. J.: Concentrations and Photochemistry of Acetaldehyde, Glyoxal, and Methylglyoxal in the  
Northwest Atlantic Ocean, *Environ. Sci. Technol.*, 53, 9512-9521, doi: 10.1021/acs.est.9b01631, 2019.
- Zöbelein, J., Sawle, S., Friedrichs, G., Ribas-Ribas, M., Lehnert, C., Paetz, K., Pflaum, M., and Waska, H.: Buoyancy and  
1085 polarity driven accumulation of dissolved organic matter in the sea surface microlayer during a phytoplankton bloom,  
*EGUsphere*, 2026, 1-32, doi: 10.5194/egusphere-2025-6563, 2026.